STIMULATED THOMSON SCATTERING

BY

ROSS LOREN SPENCER

A thesis submitted in partial fulfillment of the
requirements for the degree of

DOCTOR OF PHILOSOPHY

(Physics)

at the

UNIVERSITY OF WISCONSIN - MADISON

1979

To Margo

ACKNOWLEDGEMENTS

I thank L. W. Anderson and Jim Lawler for bringing this problem to my attention, and for many fruitful discussions. I also thank my adviser, K. R. Symon, for his careful reading of this manuscript and for many valuable discussions. I am grateful to the Danforth Foundation, the Plasma Physics Group, and the Physics Department for their support of my graduate study. Especially I thank my wife, Margo, and my children, Melanie, David, and Reed, for their patience, love, and support. I thank also my parents, Loren and LaRene Spencer, for their unfailing love and encouragement.

This research has been supported by the Danforth Foundation, by The Department of Energy, and by the Wisconsin Alumni Research Foundation, Madison, Wisconsin.

TABLE OF CONTENTS

LIST OF FIGURES

In 1917, Albert Einstein wrote a brilliant paper[2] on the connection between the Planck radiation law and the quantum mechanics of radiation. He proposed the process of stimulated emission, wherein the rate at which a system makes a radiative transition at frequency ω is proportional to the energy density of radiation evaluated at the frequency ω. He then showed that this assumption, together with the Boltzmann relation relating the relative numbers of states with different energies, implies a radiation law of the Planck form. The argument is very general, and suggests that any radiative transition can be stimulated.

In 1933, Kapitza and Dirac[3] considered the connection between Thomson's simple radiation mechanism and Einstein's stimulated emission. They calculated the effect that stimulated Thomson scattering would have on electrons shot through a pattern of standing light waves produced by coherent light reflecting onto itself from a mirror. They proposed that the effect be detected by observing the recoil of the electrons that produce the scattering. Unfortunately, the recoil is so slight that the effect is very hard to detect in this way; in fact, the experiment has never been successfully performed.

More recently, a few papers appeared which concentrated not on the effect of stimulated Thomson

scattering on the electrons, but on its effect on the amplitudes of the electromagnetic waves involved[4-9]. The usual arrangement proposed allows two counter-propagating electromagnetic waves of different frequencies to impinge on electrons. If an electron absorbs a photon from one of the waves and emits a photon into the propagation direction of the other wave, and if the electron's velocity is just right, the emitted photon will match in frequency and wave vector the photons in the second wave. Such electrons form a system capable of making a radiative transition that may be stimulated by the presence of the wave that receives the scattered photon. The process works, of course, in both directions, causing both stimulated emission and absorption in each wave. However, because of the electron recoil during absorption and emission, the velocity of an electron that causes energy transfer to one of the waves is different from the velocity that causes the inverse process to take place. If there are more electrons with one velocity than the other, there will be net energy transfer from one wave to the other. The possibility of detecting this energy transfer was at first considered to be very small because of the large coherent electromagnetic fields required. Present lasers may be capable of overcoming this difficulty, but the problem was first overcome by

replacing one of the waves by a strong helical DC magnetic field, and by replacing the stationary electrons by a high energy beam of electrons[6]. In the highly relativistic electron frame, the helical magnetic field looks like a coherent electromagnetic wave of very large amplitude. Using this idea, a group at Stanford University built a free electron amplifier[10], and subsequently a free electron laser[11], both working on the principle of stimulated Thomson scattering. The experimental results agree favorably with the quantum mechanical theories of the effect by Madey[6] and Colson[9].

The announcement that the effect discussed by Kapitza and Dirac in 1933 had at last been observed caused a great stir. Of particular interest to many investigators was a remark that appeared in a paper by Madey, Schwettman and Fairbank[12]. They pointed out that in the low energy photon limit, $\hbar\omega << m_e c^2$, the quantum mechanical formula for the gain of a wave due to stimulated Thomson scattering did not contain Planck's constant, and hence might have a classical interpretation. A few years later, Hopf, Meystre, Scully, and Louisell[13] published the first paper using classical physics to obtain the correct quantum mechanical gain formula obtained by Colson[9]. Classically, the stimulated scattering is produced by a

bunching of the radiating particles along the direction of propagation of the amplified wave. As seen from the electron frame, this bunching is produced by the non-linear ponderomotive force of the two electromagnetic waves on the electrons. It causes the transverse current driven by the two waves to be non-uniform along the propagation direction of the amplified wave. This non-uniformity produces the equivalent of an array of phased antennas; by proper choice of the frequency difference between the two waves (as observed in the electron frame), this phased array can be made to take energy from one wave, and to put it into the other. The paper of Hopf et al.[13], was accompanied by a flood of papers extending the classical results, or obtaining them in different ways[14-22].

At the same time, there was great interest in using devices with periodic magnetic fields and intense high energy electron beams, (several of which pre-dated the Stanford device), to produce stimulated radiation by other mechanisms, like stimulated Raman scattering, stimulated Brillouin scattering, and cyclotron resonance[23-38]. In these processes, the two counterpropagating electromagnetic waves are not coupled through Thomson scattering by free electrons, but through coupling to a normal mode of the electron fluid or

mechanism is shown to be analogous to non-linear Landau damping. In Chapter 5, the results are summarized. In Appendix 1, the free electron amplifier experiment is discussed, and formulas are given for transforming quantities in the highly relativistic electron frame to the laboratory frame for comparing gain coefficients. In Appendix 2, formulas for the gain and dispersion functions discussed in Chapter 3 are given. In Appendix 3, a proposed experiment to observe stimulated Thomson scattering is described. Finally, in Appendix 4 are listed useful properties of the Jacobian Elliptic Functions used in Chapter 4.

CHAPTER 2

QUANTUM MECHANICAL THEORY OF STIMULATED THOMSON SCATTERING

In this chapter is presented a quantum mechanical theory of stimulated Thomson scattering following the approach of Madey[6]. Much of the theory presented here is due to L. W. Anderson and J. E. Lawler.

Consider two oppositely directed electromagnetic waves of frequencies ω_o and ω, and of matching polarization. The wave at frequency ω_o will be called the pump wave, that at frequency ω the probe wave. Each of the two waves is assumed to be very nearly monochromatic with narrow bandwidths $\Delta\omega_o$ for the pump and $\Delta\omega$ for the probe. At time $t = 0$ they are suddenly turned on everywhere in a plasma of electron density n_e. The interaction of the waves with the electrons is allowed to last for a time τ after which it is terminated.

This rather artificial situation has for its chief virtue simplicity. The more natural physical situation would be to allow two pulses of electromagnetic radiation to pass through each other; in that case different electrons in the plasma would interact with the two waves for different times, depending on where the electrons

were when the two pulses began to overlap. This more complicated situation can be analyzed in terms of the simpler situation considered here if each pulse contains many wavelengths of the radiation, for then when the two pulses overlap in some region, locally it is as if the interaction were simultaneously turned on over many wavelengths. The simple case may then be applied locally, using the interaction time appropriate for that location, to obtain the effect on the pulses.

The stimulated scattering of photons from the pump wave to the probe wave will now be studied. The total rate of Thomson scattering into a mode, including both spontaneous and stimulated photons, is $\gamma'(n+1)$ where γ' is the rate of spontaneous Thomson scattering into the mode, and where n is the number of photons in the mode. The primary mechanism by which photons are lost from the mode is taken to be the inverse process in which the pump wave at ω_o stimulates the scattering of photons out of the probe wave at ω. Other loss mechanisms are ignored. The spontaneous rate per unit volume and per unit solid angle at which photons are Thomson backscattered from the pump wave is given by the equation

$$R = \frac{n_e r_e^2 I_o}{\hbar \omega_o} \qquad (1)$$

where r_e is the classical electron radius. In Eq. (1) use has been made of the fact that the differential Thomson scattering cross section in the backward direction is r_e^2. The backscattered frequency is $\omega' = \omega_o - 2\hbar\omega\omega_o/mc^2$ or, approximately, $\omega' \simeq \omega_o - 2\hbar\omega_o^2/mc^2$. Since the stimulated scattering lasts only for a time τ, the scattered photons will have a band width $\Delta\omega' \sim 1/\tau$ about ω'. If $\tau >> 1/\Delta\omega_o$, then the spectrum of the scattered radiation is determined solely by the interruption of the process after a time τ. Call the normalized lineshape function for the scattered radiation g. The quantity Rg is the scattering rate into all modes at the frequency ω' per unit volume per unit solid angle per unit frequency interval. Dividing Rg by $\omega'^2/(2\pi c)^3$, the number of modes per unit volume per unit solid angle per unit frequency interval will give γ', the rate of Thomson scattering from the pump wave into a mode. Hence, the scattering rate into a mode of the probe wave is given by the expression

$$\gamma' = \frac{(2\pi c)^3 R}{\omega^2} g$$

$$= \frac{8\pi^3 c^3 n_e r_e^2 I_o}{\hbar \omega^3} g(\omega - (\omega_o - 2\hbar\omega_o^2/mc^2)) \qquad (2)$$

The net gain coefficient is gotten by subtracting the rate at which the pump wave stimulates scattering out of the probe wave. Replacing ω_o and ω by $\bar{\omega} = (\omega + \omega_o)/2$ except when their difference is to be taken, and using $h\omega_o << mc^2$ yields for the net gain coefficient

$$\gamma\tau = \frac{8\pi^3 c^3 n_e r_e^2 I_o \tau}{\hbar \bar{\omega}^3} [\, g(\omega - \omega_o + 2\hbar\omega_o^2/mc^2) - g(\omega - \omega_o - 2\hbar\omega_o^2/mc^2)]$$

$$\simeq \frac{32\pi^3 n_e r_e^2 I_o c \tau}{m \bar{\omega}} \frac{d}{d\omega} g(\omega - \omega_o) \qquad (3)$$

The quantity $I\gamma\tau$ is the total change in intensity of the probe wave due to the stimulated scattering.

In the homogeneously broadened limit, where the electron gas is very cold and the spectral broadening of the Thomson scattering is the result of the finite interaction time of the electrons with the two waves the normalized lineshape, g, is given by the equation[7,9]

$$g(\omega - \omega_o) = \frac{\tau}{2\pi} \frac{\sin^2[(\omega-\omega_o)\tau/2]}{[(\omega-\omega_o)\tau/2]^2} \qquad (4)$$

and the net gain is

$$\gamma\tau = \frac{8\pi^3 n_e r_e^2 I_o c \tau^3}{m \bar{\omega}} \frac{d}{d\eta}\left(\frac{\sin^2\eta}{\eta^2}\right) \qquad (5)$$

where $\eta = (\omega - \omega_o)\tau/2$.

In an inhomogeneously broadened system, where the spectral broadening of the Thomson scattering is the result of Doppler shifts from the distribution of velocities in the electron gas, and where $f(v_z)$ is a normalized distribution function for electron velocities parallel to the light beam, the net gain is given by the equation

$$\gamma\tau = \frac{32\pi^3 n_e r_e^2 I_o c \tau}{m \bar{\omega}} \int_{-\infty}^{\infty} \frac{d}{d\omega} g(\omega - \omega_o + 2\bar{\omega}v_z/c) f(v_z) dv_z$$

$$= -\frac{16\pi^3 n_e r_e^2 I_o c^2 \tau}{m \bar{\omega}^2} \int_{-\infty}^{\infty} dv_z g(\omega-\omega_o+2\bar{\omega}v_z/c)\frac{d}{dv_z} f(v_z) \qquad (6)$$

In the limit that inhomogeneous broadening dominates over homogeneous broadening, the net gain at, or near, line center is given by the equation

$$\gamma\tau = -\frac{8\pi^3 n_e r_e^2 I_o c^3 \tau}{m \bar{\omega}^3} \frac{d}{dv_z} f(v_z) \Bigg|_{v_z = \frac{(\omega_o - \omega)c}{2\omega_o}} \tag{7}$$

For a Maxwell-Boltzmann distribution function, the net gain is given by the equation

$$\gamma\tau = \frac{8\pi^{\frac{5}{2}} n_e r_e^2 I_o c^3 \tau}{\bar{\omega}^3 k_B T} y e^{-y^2} \tag{8}$$

where

$$y = \left(\frac{mc^2}{8k_B T}\right)^{\frac{1}{2}} \frac{\omega_o - \omega}{\bar{\omega}} , \tag{9}$$

T is the temperature of the electron gas, and k_B is Boltzmann's constant. Dreicer has discussed stimulated Thomson scattering[4]. His results can be used to derive Eq. (8) except for a difference of a factor of 2π.

The gain mechanism of the free electron amplifier is essentially stimulated Thomson scattering[10]. In the free electron amplifier, a relativistic electron beam is incident on a transverse magnetic field. The field is

produced by currents in a double helix wound on a long pipe so that electrons shot down the pipe see a magnetic field whose direction rotates. When transformed to a frame of reference moving with the electrons, the spatially periodic magnetic field appears as a plane electromagnetic wave; it plays the role of the pump wave. In Appendix 1, it is shown that Eq. (5), when transformed to the highly relativistic electron frame, is the same as the gain formula for the free electron amplifier calculated by others[9,13,19,21].

Since Planck's constant does not appear in the gain coefficient of the free electron laser, a classical approach might be expected to give the same result. This was first suggested by Madey et al[12]. Since that suggestion, many papers have appeared exploring the classical interpretation of both the free electron laser and stimulated Thomson scattering[8,15,20,30,42,54,60-62]. In the remainder of this thesis, a classical calculation is presented that yields the gain and dispersion of a plasma in the presence of two counter-propagating electromagnetic waves. The gain formula so obtained agrees, in the unsaturated limit, with that obtained quantum mechanically in this chapter. In addition, the classical calculation shows the relationship between stimulated Thomson scattering and stimulated Raman

scattering, and how the effect saturates by non-linear Landau damping.

CHAPTER 3

FLUID THEORY OF STIMULATED THOMSON SCATTERING

A. Introduction

In this chapter a fluid calculation will be described that yields the same formula for the gain coefficient as that obtained quantum mechanically in Chapter 2. In addition, the close relationship between stimulated Thomson scattering and stimulated Raman scattering is clarified, and the effect of damping in the fluid equations on the gain coefficient is obtained. Besides the gain coefficient, the dispersion due to stimulated Thomson scattering is also obtained.

In spite of being able to take the limit of stimulated Raman scattering, namely $\omega_o - \omega = \omega_p$, the results obtained here are difficult to compare with the rather large literature on this subject (see for example Refs. 44 and 51). One of the reasons for this difficulty is that the usual approach is to Fourier transform the equations in space and time, whereas in this chapter an initial value problem is solved. This procedure produces transient solutions, and it is these transients that are of interest in connection with

stimulated Thomson scattering. A second reason is that in Raman scattering an incident electromagnetic wave decays into a plasma wave and a scattered electromagnetic wave. Here, two externally produced electromagnetic waves are incident on a plasma and act to induce a plasma wave if the resonance condition is satisfied. Thus, the approach taken here is more in the spirit of optical mixing of electromagnetic waves or of beat heating in plasmas[30,33,35,37,39,41,43,50,51,64].

B. A Perturbation Expansion of the Electron Fluid Equations and Maxwell's Equations

It is assumed that two counterpropagating electromagnetic waves of the same polarization are incident on a neutralized electron fluid. At time t=0 the two waves are instantaneously turned on, everywhere in space, in the previously undisturbed fluid. Effects due to the sudden turning on are ignored. The development in time of the intensities and relative phases of the two waves are obtained by solving the electron fluid equations and Maxwell's equations. It is assumed that the timescale for the amplitudes and phases of the waves to change is much longer than the period of either of the two waves, and in fact is much longer than

$1/\delta\omega$, where $\delta\omega = \omega_o - \omega$. The vector potential describing the two waves is written in the form

$$\vec{A}_T = [\ \frac{c}{\omega_o} E_o\ (1 + \theta_o(t))\ \sin(\ k_o z - \omega_o t + \phi_o(t)\ ) + \frac{c}{\omega} E\ (1 + \theta(t)\ )\ \sin(\ kz + \omega t + \phi(t)\ )\ ]\ \hat{x} \tag{10}$$

where θ and θ_o represent the change in the wave amplitudes and where ϕ and ϕ_o represent the change in the phases of the waves. Note that $\vec{A}_T$ satisfies the Coulomb gauge condition, $\vec{\nabla}\cdot\vec{A}_T = 0$. At time t=0, θ, ϕ, θ_o, and ϕ_o are all zero. These quantities are assumed to satisfy the following ordering.

$$\dot{\theta},\ \dot{\phi},\ \dot{\theta}_o,\ \dot{\phi}_o \ll \delta\omega \tag{11}$$

The electron fluid is taken to be described by the equation of motion,

$$\frac{\partial\vec{v}}{\partial t} + \vec{v}\cdot\nabla\vec{v} = -\frac{e}{m}(\ \vec{E} + \frac{\vec{v}}{c} \times \vec{B}\ ) - \frac{1}{mn}\vec{\nabla} p \tag{12}$$

the equation of continuity,

$$\frac{\partial n}{\partial t} + \vec{\nabla}\cdot(\ n\vec{v}\ ) = 0 \tag{13}$$

an equation of state,

$$\left(\frac{p}{p_o} \right) = \left(\frac{n}{n_o} \right)^{\gamma^*} \tag{14}$$

and Maxwell's equations,

$$\vec{\nabla} \cdot \vec{E} = -4\pi e \left(n - n_o \right) \tag{15}$$

$$\vec{\nabla} \cdot \vec{B} = 0 \tag{16}$$

$$\vec{\nabla} \times \vec{B} = -\frac{4\pi}{c} e n \vec{v} + \frac{1}{c} \frac{\partial \vec{E}}{\partial t} \tag{17}$$

$$\vec{\nabla} \times \vec{E} = -\frac{1}{c} \frac{\partial \vec{B}}{\partial t} \tag{18}$$

The quantity $\vec{v}$ is the fluid velocity, p is the pressure, n is the electron fluid density, m is the electron mass, and $\vec{E}$ and $\vec{B}$ are the electric and magnetic fields. The variable γ^* represents the adiabatic exponent and n_o is the density of the neutralizing positive charge. There is a wealth of information contained in these equations. For the purposes of this calculation, it is sufficient to make a perturbation expansion of the equations. To lowest order, the fluid is taken to respond only to the electric fields of the two external electromagnetic waves; in the next order, the motion of the fluid along

the z-direction, the direction of propagation of the waves, is considered. Hence, the following perturbation scheme is adopted.

$$\vec{v} = \vec{v}_o + \delta v\, \hat{z} \tag{19}$$

$$n = n_o + \delta n \tag{20}$$

$$\vec{E} = \vec{E}_T + \delta E\, \hat{z} \tag{21}$$

$$\vec{B} = \vec{B}_T \tag{22}$$

The quantity $\vec{v}_o$ is the fluid velocity driven by the external electric fields while δv, δn, and δE describe the motion of the fluid in the z-direction and the longitudinal electric field produced by that motion.

Equations (19)-(22) are substituted into the fluid equations and Maxwell's equations, Eqs.(15)-(18), and the system of equations is linearized to obtain the set of equations

$$\frac{\partial \vec{v}_o}{\partial t} = -\frac{e}{m}\vec{E}_T \tag{23}$$

$$\frac{\partial \delta v}{\partial t} = -\frac{e}{mc}\left(\vec{v}_o \times \vec{B}_T\right)_z - \frac{e}{m}\delta E - \frac{\gamma^* k_B T}{m n_o}\frac{\partial \delta n}{\partial z} \tag{24}$$

$$\frac{\partial \delta E}{\partial z} = -4\pi e\, \delta n \tag{25}$$

$$\frac{\partial^2}{\partial z^2}\vec{A}_T - \frac{1}{c^2}\frac{\partial^2}{\partial t^2}\vec{A}_T - \frac{\omega_p^2}{\omega^2}\vec{A}_T = \frac{4\pi}{c} e\, \delta n \vec{v}_o \tag{26}$$

(27)

This procedure is similar to that followed in Refs. 38 and 64. In obtaining these equations it was assumed that the fluid and the fields are homogeneous in the x- and y-directions so that all derivatives with respect to x and y vanish.

C. The Motion of the Electron Fluid Driven by the Ponderomotive Force for Weak Plasma Response

With the ordering of Eq. (11), this set of equations may be solved by iteration: find the perturbed fluid quantities assuming that θ, θ_o, ϕ, and ϕ_o are negligible,

then substitute the perturbed fluid quantities into the wave equation, Eq. (27), to determine θ, θ_o, ϕ, and ϕ_o. Equation (23) is solved first to obtain

$$\vec{v}_o = \frac{e}{mc}\left(\vec{A}_T - \vec{A}_T\Big|_{t=0} \right) \qquad (28)$$

Note that the requirement that the fluid be initially undisturbed has been applied. This expression for $\vec{v}_o$ is substituted into the right hand side of Eq. (24). The term containing $\vec{v}_o$ in Eq. (24) acts as an external driving force in the longitudinal equation of motion, and is simply the familiar ponderomotive force together with a term due to the initial conditions:

$$-\frac{e}{mc}\vec{v}_o \times \vec{B}_T = -\frac{e^2}{2m^2c^2}\vec{\nabla} A_T^2 + \frac{e^2}{m^2c^2}\vec{A}_T\Big|_{t=0} \times (\vec{\nabla}\times\vec{A}_T) \qquad (29)$$

The ponderomotive force is the force that produces stimulated Thomson scattering, and must be treated with care. The importance of the ponderomotive force may be seen by expanding A_T^2 in the following way.

$$A_T^2 = E_o^2 \frac{c^2}{\omega_o^2} \sin^2(k_o z - \omega_o t) + E^2 \frac{c^2}{\omega^2} \sin^2(kz + \omega t)$$

$$+ \frac{E_o E\, c^2}{\omega\, \omega_o} [\cos((k_o-k)z-(\omega_o+\omega)t) - \cos((k_o+k)z-\delta\omega t)] \qquad (30)$$

The first three terms in this expression are high phase velocity terms and can have little effect on the electron motion, but the fourth term has phase velocity much less than the speed of light; it can influence the electron fluid more strongly than the other terms. Assuming that the high phase velocity terms in Eq. (30) as well as similar terms arising from the initial value term in Eq. (29) are negligible, the ponderomotive force term in the fluid equation of motion may be written in the form

$$\frac{\vec{F}_p}{m} = - \frac{e}{mc}(\vec{v}_o x \vec{B}_T) \simeq - \frac{1}{2} \frac{\Omega^2 c}{\bar{\omega}} \sin((k_o+k)z - \delta\omega t) \hat{z} \qquad (31)$$

where $$\Omega^2 = \frac{(k_o+k)\, e^2\, EE_o}{m^2\, c\, \bar{\omega}} \simeq \frac{2E_o E\, e^2}{m^2\, c^2}$$

and where $\bar{\omega} = (\omega + \omega_o)/2$. Substituting this term into Eq. (24) and Fourier transforming Eqs. (24)-(26) in z with respect to the Fourier transform variable k' yields the following set of equations.

$$\frac{\partial}{\partial t}\,\tilde{\delta v} = \frac{\tilde{F}_p}{m} - \frac{e}{m}\,\tilde{\delta E} - \frac{i\,k'\,\gamma^*\,k_B T}{m\,n_o}\,\tilde{\delta n} \qquad (32)$$

$$\frac{\partial}{\partial t}\,\tilde{\delta n} + ik'\,n_o\tilde{\delta v} = 0 \qquad (33)$$

$$ik'\,\tilde{\delta E} = -\,4\pi e\,\tilde{\delta n} \qquad (34)$$

Combining these equations yields the single equation for δn,

$$\frac{d^2}{dt^2}\,\tilde{\delta n} + \left(\omega_p^2 + \frac{\gamma^* k_B T}{m}\,k'^2\right)\tilde{\delta n} = -\frac{ik'n_o}{m}\,\tilde{F}_p \qquad (35)$$

The left hand side by itself would simply yield the familiar Bohm-Gross dispersion relation for plasma waves. The right hand side represents the effect of the low frequency part of the non-linear ponderomotive force. Mathematically, the equation is simply that describing the driven harmonic oscillator.

Equation (35) does not include any damping effects. Since plasma waves may be damped either collisionally or

by Landau damping, a phenomenological damping term is added to Eq. (35) to obtain the equation

$$\frac{d^2}{dt^2}\,\tilde{\delta n} + \Gamma \frac{d}{dt}\,\tilde{\delta n} + \omega'^2\,\tilde{\delta n} =$$

$$\frac{k'}{4}\frac{n_o \Omega^2 c}{\bar{\omega}}\left[\,\delta(k'-k_o-k)\,e^{-i\delta\omega t} - \delta(k'+k_o+k)\,e^{i\delta\omega t}\,\right] \qquad (36)$$

where $\omega'^2 = \omega_p^2 + \frac{\gamma^* k_B T}{m}(k_o+k)^2$

Equation (36) is simply solved, but working with its solutions is very messy. However, the technique used to find the time dependent electromagnetic field amplitudes and phases can be illustrated in a very simple case which is interesting in its own right. The more complicated results obtained by working with Eq. (36) are given in Appendix 2 and in the figures. The simple case is to assume that Γ and ω' are both zero. In this case Eq. (36) can be immediately integrated to obtain

$$\tilde{\delta n} = -\frac{k' n_o{}^2 c}{4\delta\omega^2\,\bar{\omega}}\left[\,\delta(k'-k_o-k)\,e^{-i\delta\omega t} - \delta(k'+k_o+k)\,e^{i\delta\omega t}\,\right] + Ct + D \qquad (37)$$

where C and D are constants. That the fluid be initially undisturbed imposes the conditions

$$\tilde{\delta n}\Big|_{t=0} = 0 \qquad (38)$$

$$\frac{d}{dt}\tilde{\delta n}\Big|_{t=0} = 0 \qquad (39)$$

which determine C and D. Equation (37) is now inverse-Fourier transformed in k' to obtain the desired solution.

$$\delta n = -\frac{n_o \Omega^2}{\delta\omega^2}\left[\cos\left((k_o+k)z - \delta\omega t\right)\right. \qquad (40)$$

$$\left. - \delta\omega t \sin(k_o+k)z - \cos(k_o+k)z\right]$$

D. The Gain and Dispersion of the Waves

Having solved for the fluid motion, the electromagnetic fields may now be determined. Substituting Eq. (10) into the wave equation, Eq. (27), and applying the ordering of Eq. (11) gives for Eq. (27)

$$\left[\left(-\frac{k_o^2 c}{\omega_o} + \frac{\omega_o}{c} - \frac{\omega_p^2}{c\omega_o} \right) - \frac{2\dot{\phi}_o}{c} \right] E_o \sin(k_o z - \omega_o t + \phi_o)$$

$$+ \frac{2E_o}{c} \dot{\theta}_o \cos(k_o z - \omega_o t + \phi_o)$$

$$+ \left[\left(-\frac{k^2 c}{\omega} + \frac{}{c} - \frac{\omega_p^2}{c\omega} \right) + \frac{2\dot{\phi}}{c} \right] E \sin(kz + \omega t + \phi) \qquad (41)$$

$$- \frac{2E}{c} \dot{\theta} \cos(kz + \omega t + \phi) = \frac{4\pi}{c} e \, \delta n \, v_{ox}$$

Expressions for θ, ϕ, θ_o, and ϕ_o may be obtained by multiplying Eq. (41) by an appropriate factor and integrating over time and space. The time integration is assumed to be over a time, t, long compared to the wave period of either wave, but short compared to the time $1/\delta\omega$. The integration in z is taken to be over a region long compared with the length $1/(k-k_o)$. The procedure is illustrated by multiplying Eq. (41) by $\cos(kz)\cos(\omega t)$ and integrating as described above. Equation (41) becomes

$$-\frac{E}{2c}\dot{\theta} = \frac{4\pi}{c} e \frac{1}{Lt} \int_{-L/2}^{L/2} dz \int_0^t dt' \; \delta n \, v_{ox} \cos kz \cos\omega t' \qquad (42)$$

Multiplying by $\cos(kz)\sin(\omega t)$ and integrating yields

$$\frac{1}{4}\left(-\frac{k^2c}{\omega} + \frac{\omega}{c} - \frac{\omega_p^2}{c\omega} \right) E + \frac{E}{2c}\dot{\phi} =$$

$$\frac{4\pi}{c} e \frac{1}{Lt} \int_{-L/2}^{L/2} dz \int_0^t dt' \quad \delta n \, v_{ox} \cos kz \sin\omega t' \tag{43}$$

Carrying out the operations on the right hand sides of Eqs. (42) and (43), and equating terms of like order, yields the familiar dispersion relation for electromagnetic waves in a plasma and differential equations for θ and ϕ.

$$\omega^2 = \omega_p^2 + k^2c^2 \tag{44}$$

$$\dot{\theta} = \frac{4\pi^2 n_o r_e^2 I_o c}{m \bar{\omega}} P(t) \tag{45}$$

$$\dot{\phi} = -\frac{4\pi^2 n_o r_e^2 I_o c}{m \bar{\omega}} Q(t) \tag{46}$$

where

$$P = \frac{4}{\delta\omega^2} \left(\sin\delta\omega t - \delta\omega t \cos\delta\omega t \right) \tag{47}$$

$$Q = \frac{4}{\delta\omega^2} \left(\cos\delta\omega t - 1 + \delta\omega t \sin\delta\omega t \right) \tag{48}$$

$$I_o = \frac{c}{8\pi} E_o^2 \tag{49}$$

The differential equations are easily integrated over the time of interaction, τ , to obtain

$$\theta = \frac{4\pi^2 n_o r_e^2 I_o c}{m \bar{\omega}} J \tag{50}$$

$$\phi = - \frac{4\pi^2 n_o r_e^2 I_o c}{m \bar{\omega}} K \tag{51}$$

where

$$J = \tau^3 \frac{d}{d\eta} \left(\frac{\sin^2\eta}{\eta^2} \right) \tag{52}$$

$$K = \tau^3 \frac{d}{d\eta} \left(\frac{1}{\eta} - \frac{\sin 2\eta}{2\eta^2} \right) \tag{53}$$

and where $\eta = -\delta\omega\tau/2$.

The functions J and K given above are displayed in Figures 1 and 2.

A similar calculation shows that

Figure 1

The Gain Curve for Unsaturated
Stimulated Thomson Scattering

The function $-J(\eta) = -\tau^3 \frac{d}{d\eta}\left(\frac{\sin^2\eta}{\eta^2}\right)$ is displayed for $\tau = 1$.

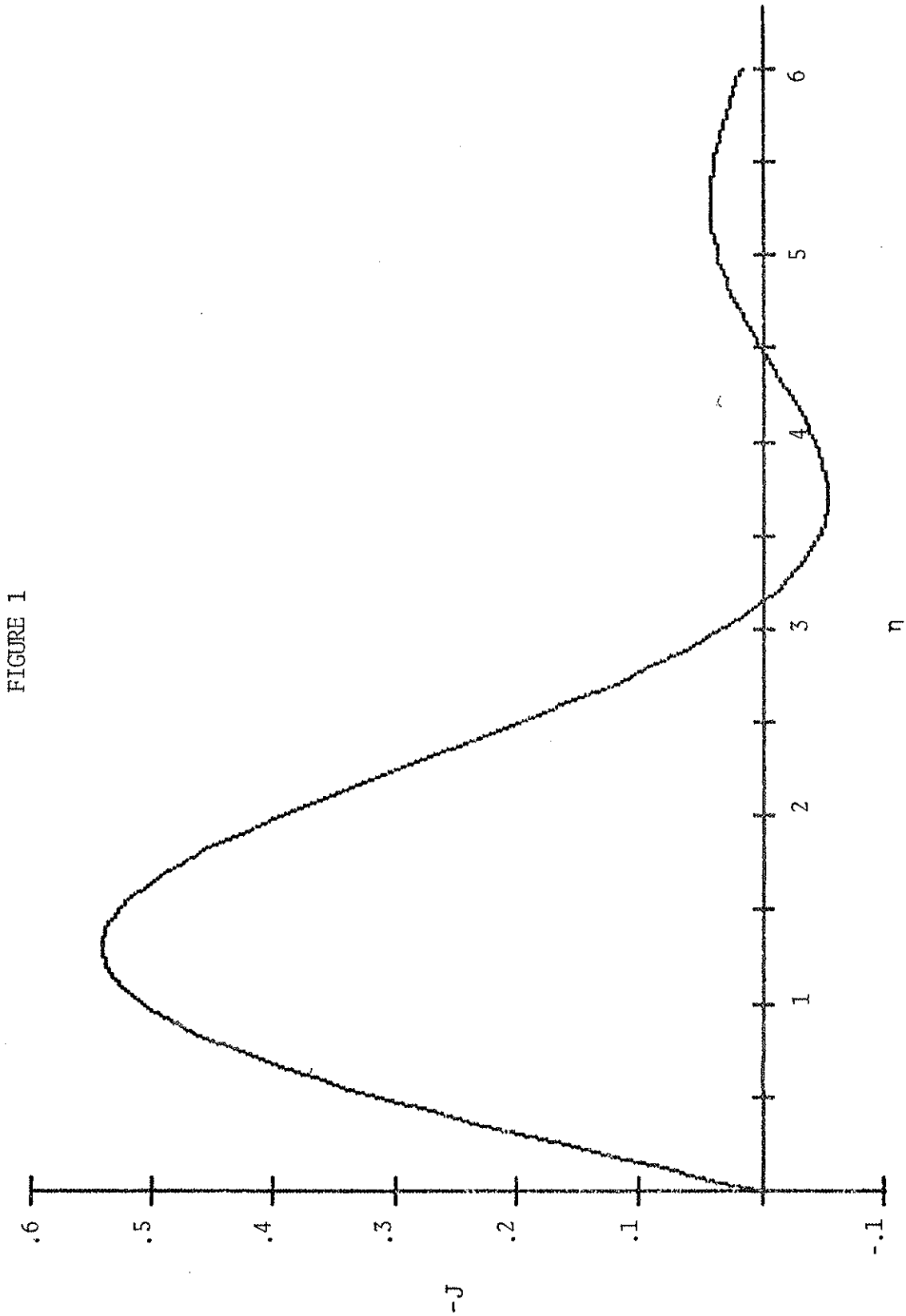

FIGURE 1

Figure 2

The Dispersion Curve for Unsaturated
Stimulated Thomson Scattering

The function $K(\eta) = \tau^3 \frac{d}{d\eta} \left(\frac{1}{\eta} - \frac{\sin 2\eta}{2\eta^2} \right)$ is displayed for $\tau = 1$.

FIGURE 2

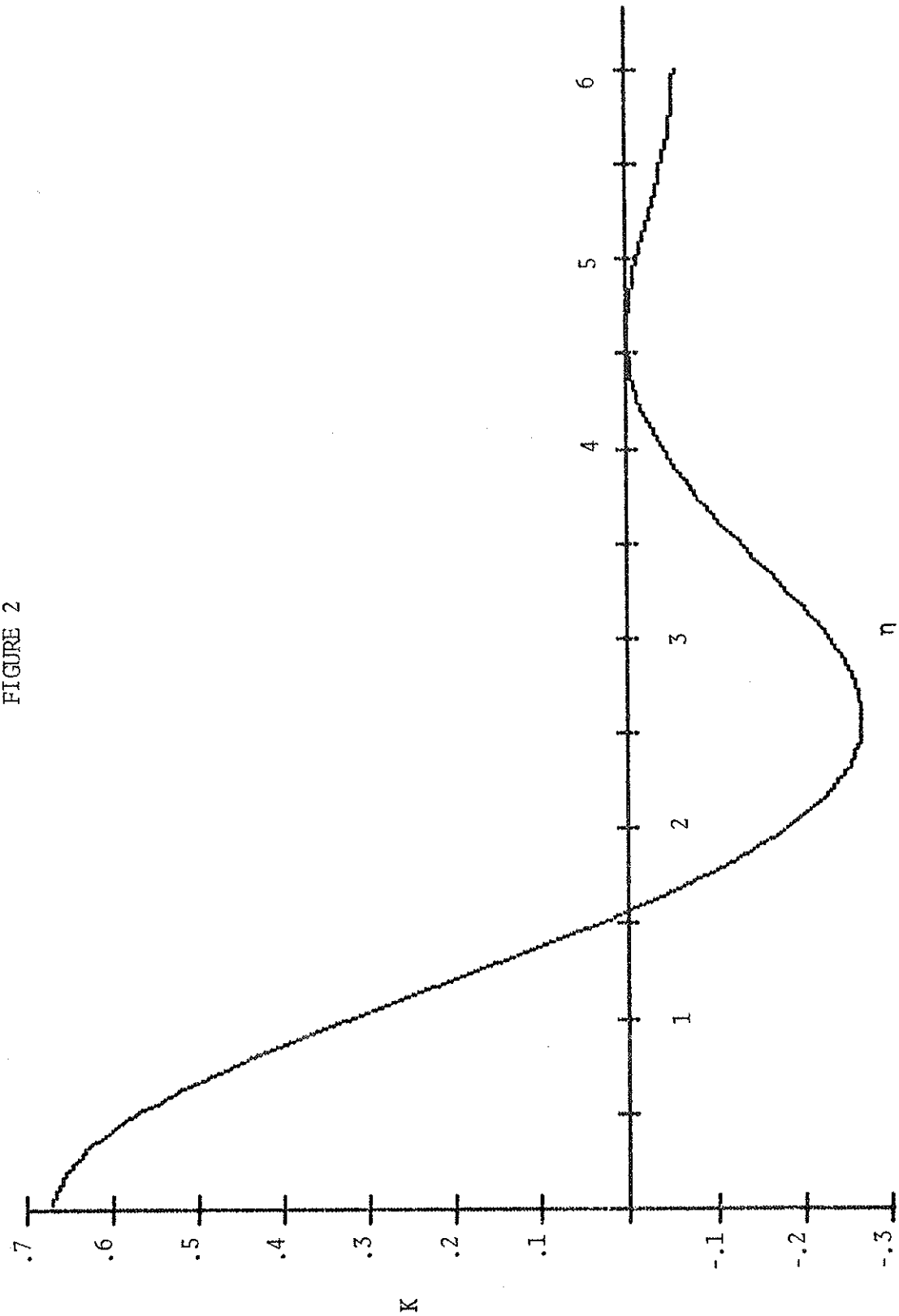

$$E_o^2 \theta_o = - E^2 \theta \qquad (54)$$

$$E_o^2 \phi_o = - E^2 \phi \qquad (55)$$

Equation (54) shows that energy is conserved between the two waves; to the order of approximation taken here, the fluid acts only to transfer energy from one wave to the other. This is not strictly true, of course, for the fluid obviously gains energy in the process described above. The amount of energy gained by the fluid is of order $\delta\omega/\bar{\omega}$ compared with the energy transferred between the two waves. Terms of this order have been consistently neglected in this calculation.

E. Comparison with the Quantum Mechanical Result; The Kramers-Kronig Relations

To make the connection between Eq. (50) and the quantum mechanical result, note that γ_T given in Eq. (5) represents the fractional gain in intensity due to stimulated Thomson scattering acting for a time τ. Since $I \alpha E^2(1 + 2\theta)$,

$$\gamma\tau = 2\theta = \frac{8\pi^2 n_o r_e^2 I_o c \tau^3}{m \bar{\omega}} \frac{d}{d\eta}\left(\frac{\sin^2\eta}{\eta^2} \right) \qquad (56)$$

in agreement with the quantum mechanical result.

The time derivatives of θ and ϕ may be given an interpretation as real and imaginary parts of a non-linear index of refraction. Since $\dot{\theta}$ and $\dot{\phi}$ are small and vary slowly in time compared to ωt, and since $(1 + \theta) \simeq \exp(\theta) = \exp(\int_0^\tau \dot{\theta}\, dt\ )$, the vector potential of the probe wave can be expressed as follows.

$$\vec{A} = \frac{c}{\omega} \vec{E}\, e^{i(kz + \int_0^\tau \omega^* dt)} \qquad (57)$$

where $\omega^* = \omega + \dot{\phi} - i\dot{\theta}$

The index of refraction may now be written in the form

$$n^2 = \frac{k^2 c^2}{\omega^{*2}} \simeq 1 - \frac{\omega_p^2}{\omega^2} - \frac{2\dot{\phi}}{\omega} + \frac{2i\dot{\theta}}{\omega} \qquad (58)$$

It is interesting to note that $\dot{\theta}$ and $\dot{\phi}$, interpreted in this way, are connected by the Kramers-Kronig relations with respect to ω. The Kramers-Kronig relations apply to linear, time independent systems, and hence might not be expected to apply to the situation

considered here. The question of linearity is answered by noting that although the interaction of the two waves is non-linear, it is non-linear in a special way. The interaction is characterized by the quantity $\Omega^2 \alpha EE_o$; this is a non-linear term, but is linear separately in the unperturbed amplitudes E and E_o. Another way of saying the same thing is to say that the medium seen by the probe wave consists of the electrons plus the pump wave. Viewed in this way, the interaction of the probe wave with the "medium" is linear. The problem that the medium is time dependent is solved by showing that the same results are obtained from a different, albeit contrived, medium which is time independent. Note that Equation (36) is linear in the density of the medium, n_o, and in the density perturbation δn. Suppose now that instead of one medium of density n_o, there are many such media of smaller densities in the presence of the two waves. At some time, one of the media has all of its density perturbations smoothed out. It is then allowed to respond for a time τ, at which time it is once again made smooth and allowed to respond again for a time τ. The same thing happens over and over for all of the media, but the smoothing times for the various media are randomly scattered over the time interval τ. At the end of each time interval, the medium which is smoothed out

will have produced a change in the probe wave amplitude. From Eq. (57), the change can be represented, for small ϕ, by

$$\Delta\vec{E} = \vec{E}\, e^{i(kz+\omega t)} \,(\theta + i\phi) \qquad (59)$$

Thus for this system, θ and ϕ are simply the real and imaginary parts of the linear response function for the probe wave. They are to be thought of as functions of ω with ω_o and τ as parameters. When viewed in this way, it is clear that θ and ϕ should be connected by the Kramers-Kronig relations. Since these relations are linear relations between analytic functions, and since τ is simply a parameter, $\dot{\theta}$ and $\dot{\phi}$ should also be connected by the Kramers-Kronig relations.

F. The Gain and Dispersion for General Plasma Response

The effect of including nonzero ω' and Γ will now be considered. Equation (36) is easy, if messy, to solve. The solution for δn is combined with $\vec{v}_o$ to obtain the non-linear correction to the transverse current, and hence to obtain θ, ϕ, θ_o, and ϕ_o from the procedure outlined in Eqs. (42)-(53). Carrying out this program

yields more complicated expressions for J and K. These expressions, together with the solution of Eq. (36) for δn are given in Appendix 2.

Two cases will now be considered. In case (i) the interaction time τ is held fixed, as are Γ and ω', while $\delta\omega$ is allowed to vary. In case (ii), the difference frequency, $\delta\omega$, Γ, and ω' are held fixed while τ is allowed to vary. Case (i) is obtained in arrangements like the free electron amplifier experiment where the difference frequency is varied by changing the electron beam energy while the other parameters are held fixed. In case (ii) the time development of the amplitudes and phases of the electromagnetic waves is considered, a natural thing to look at given the way the problem has been solved.

Figures 3-8 show the functions J and K for case (i) with $\tau = 1$ and with $0 \leq \delta\omega\tau \leq 12$. Note that in all cases the maximum gain occurs for $\omega'\tau << 1$ and $\Gamma\tau << 1$, i.e. for simple stimulated Thomson scattering. Note also that there is very little difference between the cases of critical damping and overdamping of the plasma wave. If τ has a value other than $\tau = 1$, the following identity allows the desired value of J or K to be found in terms of the case $\tau = 1$.

Figure 3

The Gain Curve for Underdamping and τ Fixed

The function J is displayed vs. $\delta\omega\tau$ for $\tau = 1$, for $\Gamma \ll \omega'$, and for 3 values of ω':

———— $\Gamma = .0001 \quad \omega' = .001$

— — — $\Gamma = .001 \quad \omega' = 2$

—— —— $\Gamma = .001 \quad \omega' = 4$

FIGURE 3

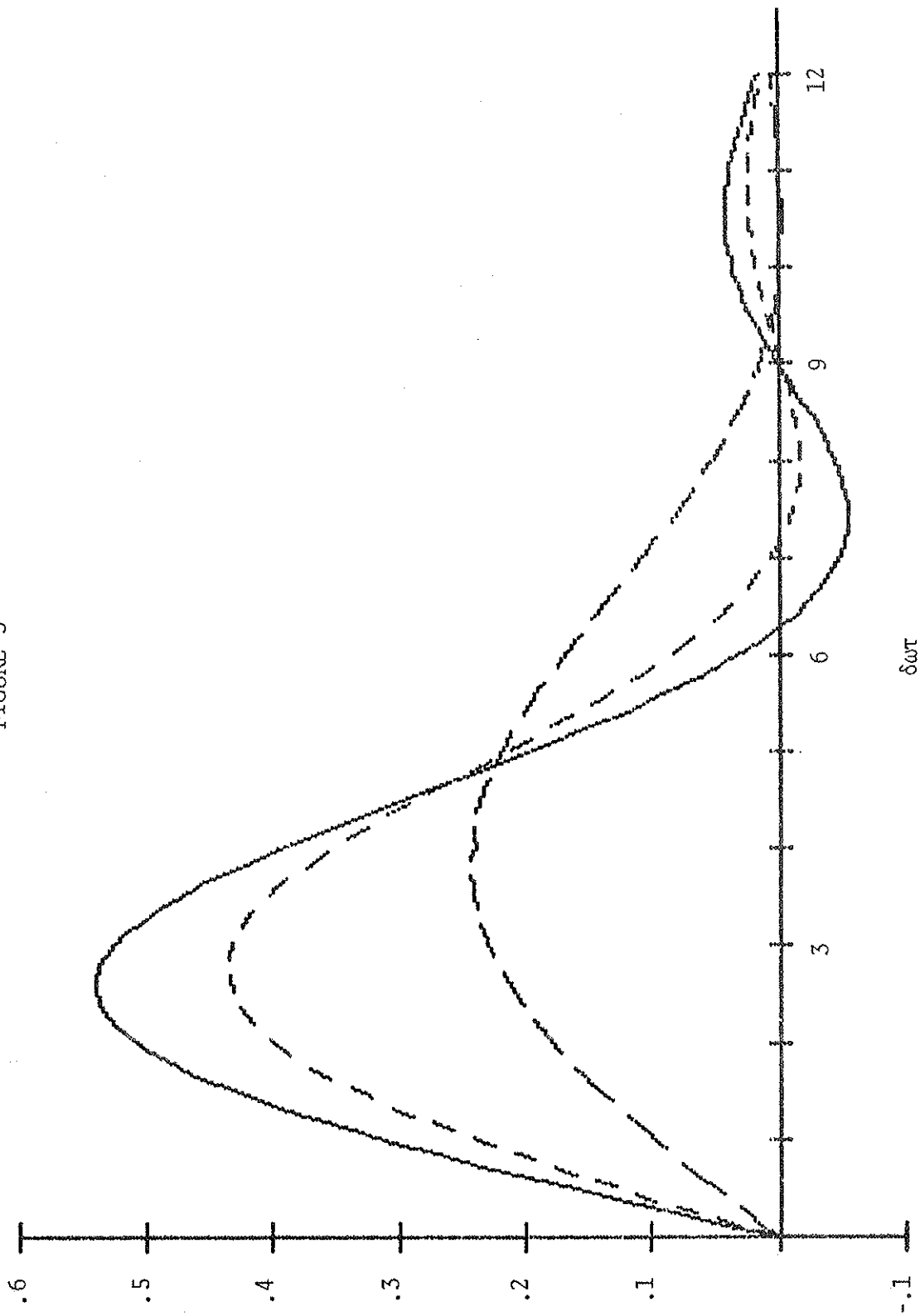

Figure 4

The Gain Curve for Critical Damping and τ Fixed

The function J is displayed vs. $\delta\omega\tau$ for $\tau = 1$, for $\omega' = \frac{1}{2}\Gamma$, and for 3 values of Γ:

———— $\Gamma = .019 \quad \omega' = .01$

— — — $\Gamma = 1.999 \quad \omega' = 1$

—— —— $\Gamma = 3.999 \quad \omega' = 2$

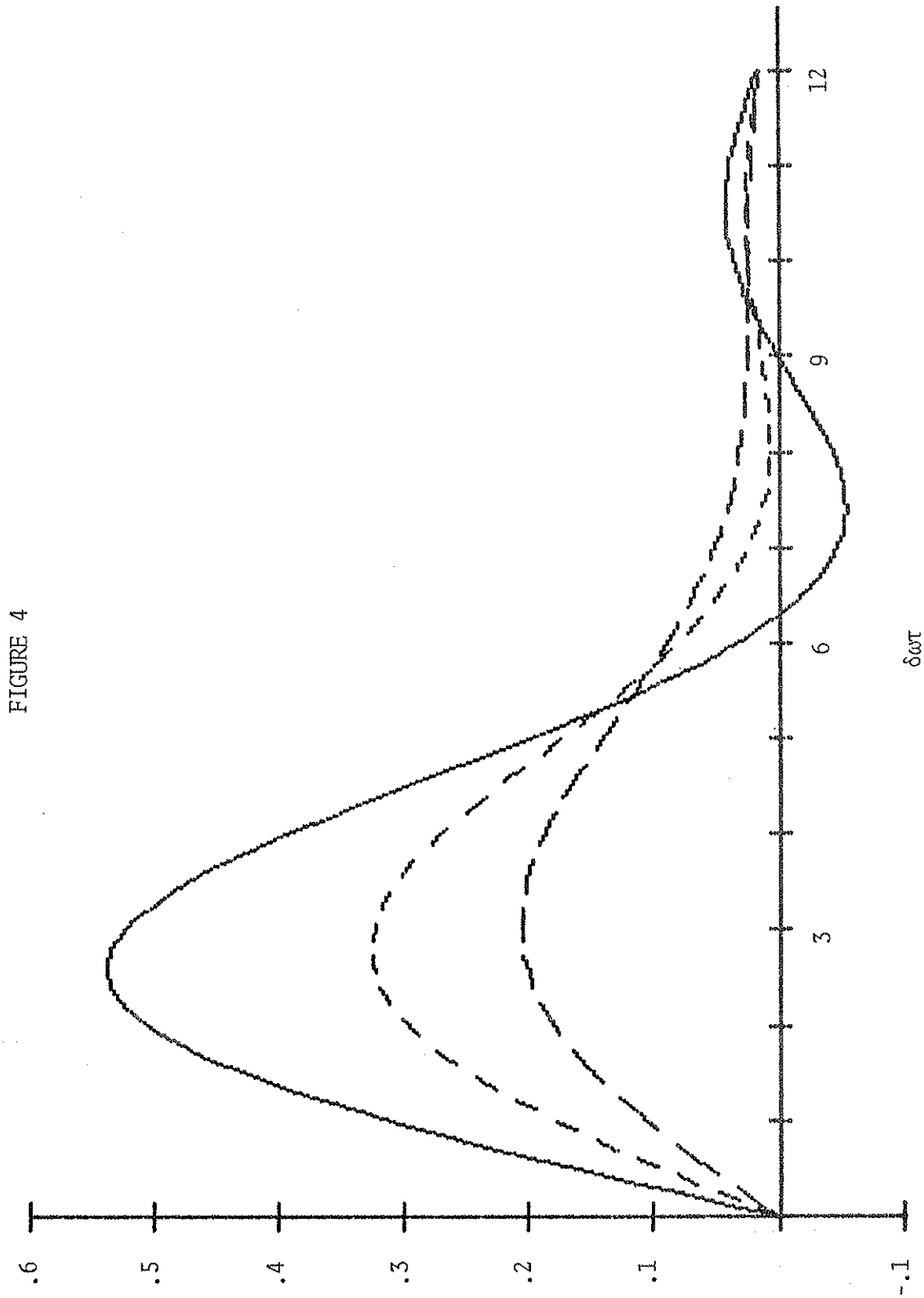

FIGURE 4

Figure 5

The Gain Curve for Overdamping and τ Fixed

The function J is displayed vs. $\delta\omega\tau$ for $\tau = 1$, for $\omega' \ll \Gamma$, and for 3 values of Γ:

———— $\Gamma = .002$ $\omega' = .0001$

— — — $\Gamma = 2$ $\omega' = .01$

—— —— $\Gamma = 4$ $\omega' = .01$

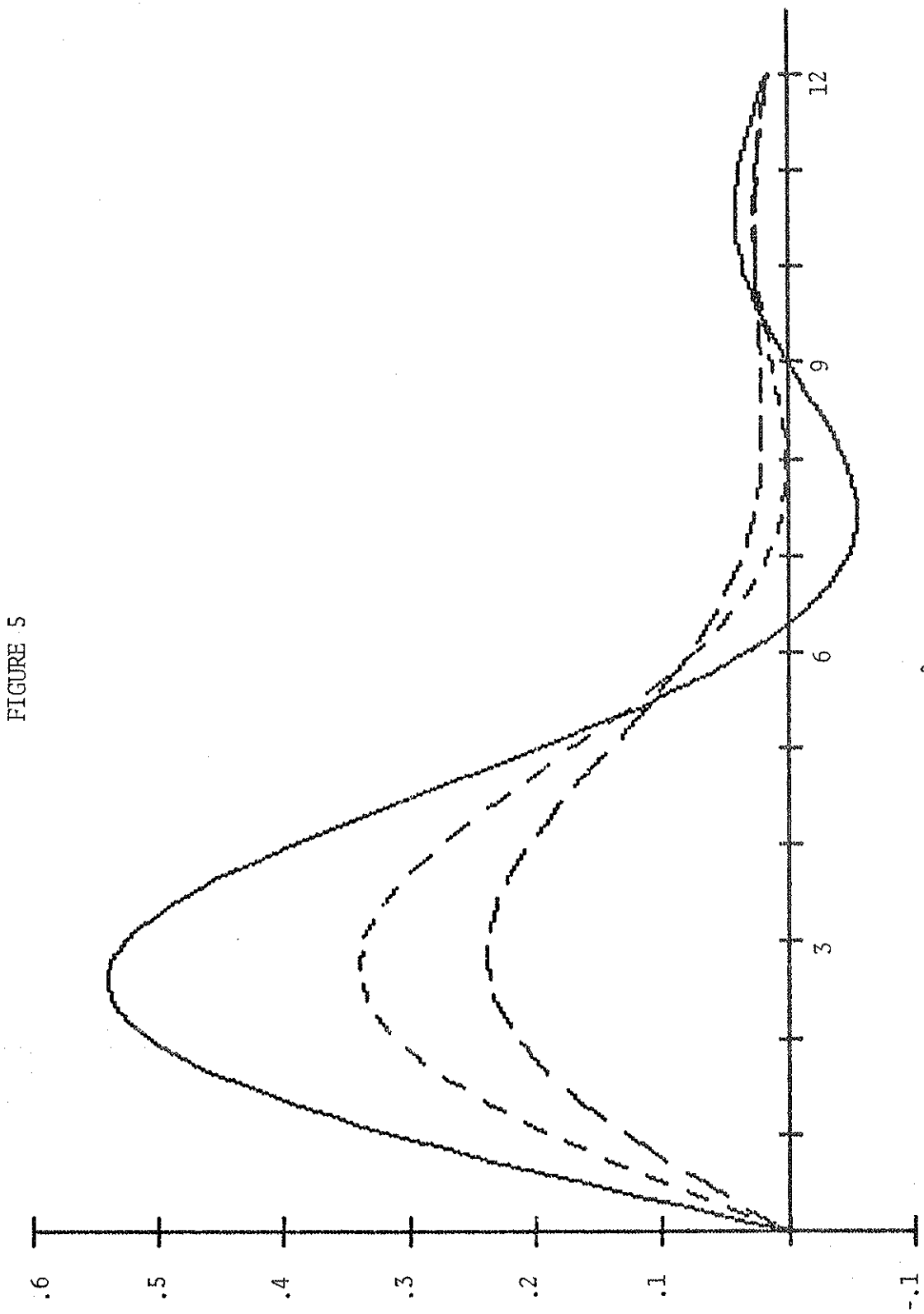

FIGURE 5

Figure 6

The Dispersion Curve for Underdamping and τ Fixed

The function K is displayed vs. $\delta\omega\tau$ for $\tau = 1$, for $\Gamma \ll \omega'$, and for 3 values of ω':

———— $\Gamma = .001 \quad \omega' = .01$

— — — $\Gamma = .001 \quad \omega' = 2$

—— —— $\Gamma = .001 \quad \omega' = 4$

FIGURE 6

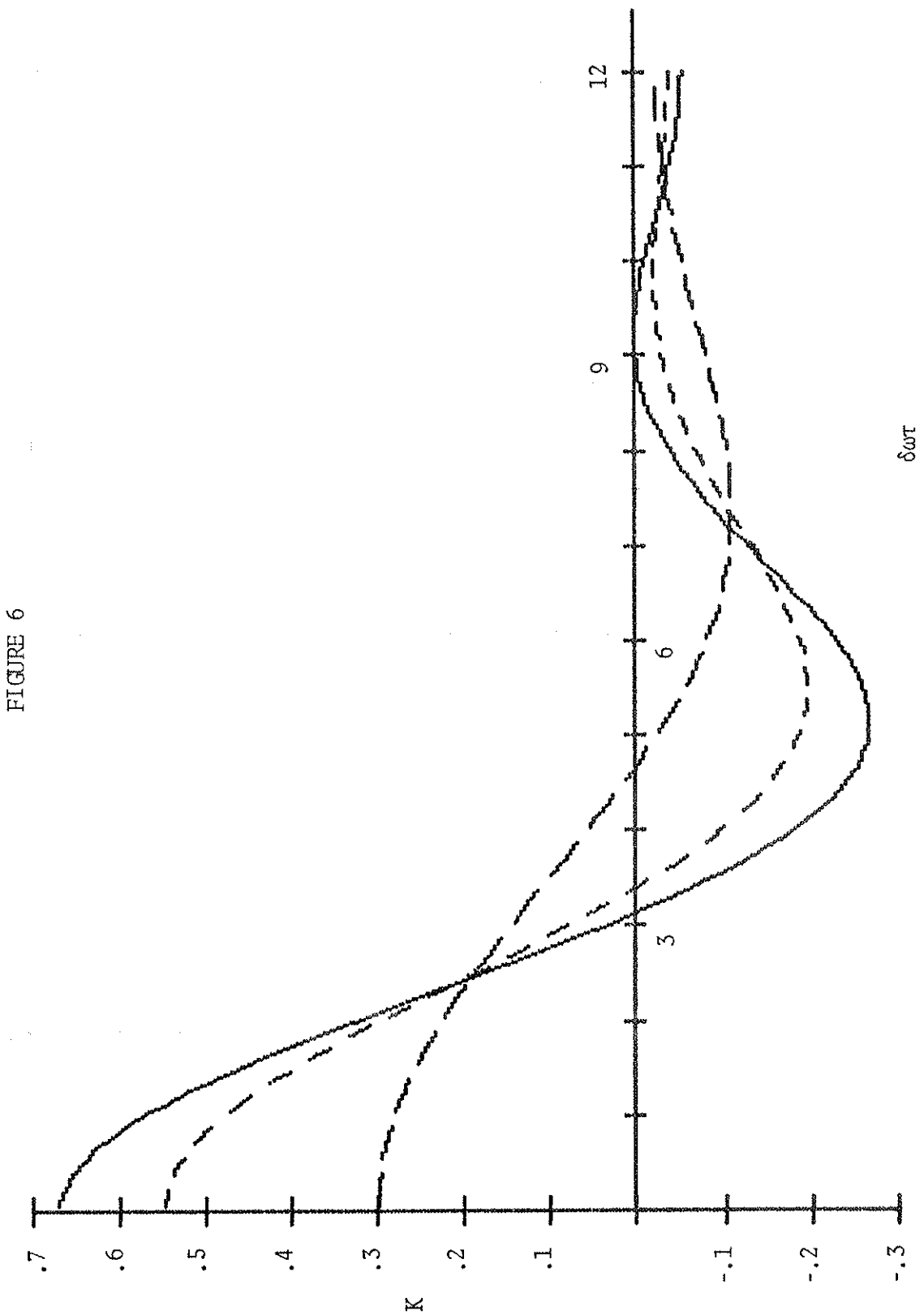

Figure 7

The Dispersion Curve for Critical Damping and τ Fixed

The function K is displayed vs. $\delta\omega\tau$ for $\tau = 1$, for $\omega' = \frac{1}{2}\Gamma$, and for 3 values of Γ:

———— $\Gamma = .19 \quad \omega' = .1$

— — — $\Gamma = 1.99 \quad \omega' = 1$

—— —— $\Gamma = 3.99 \quad \omega' = 2$

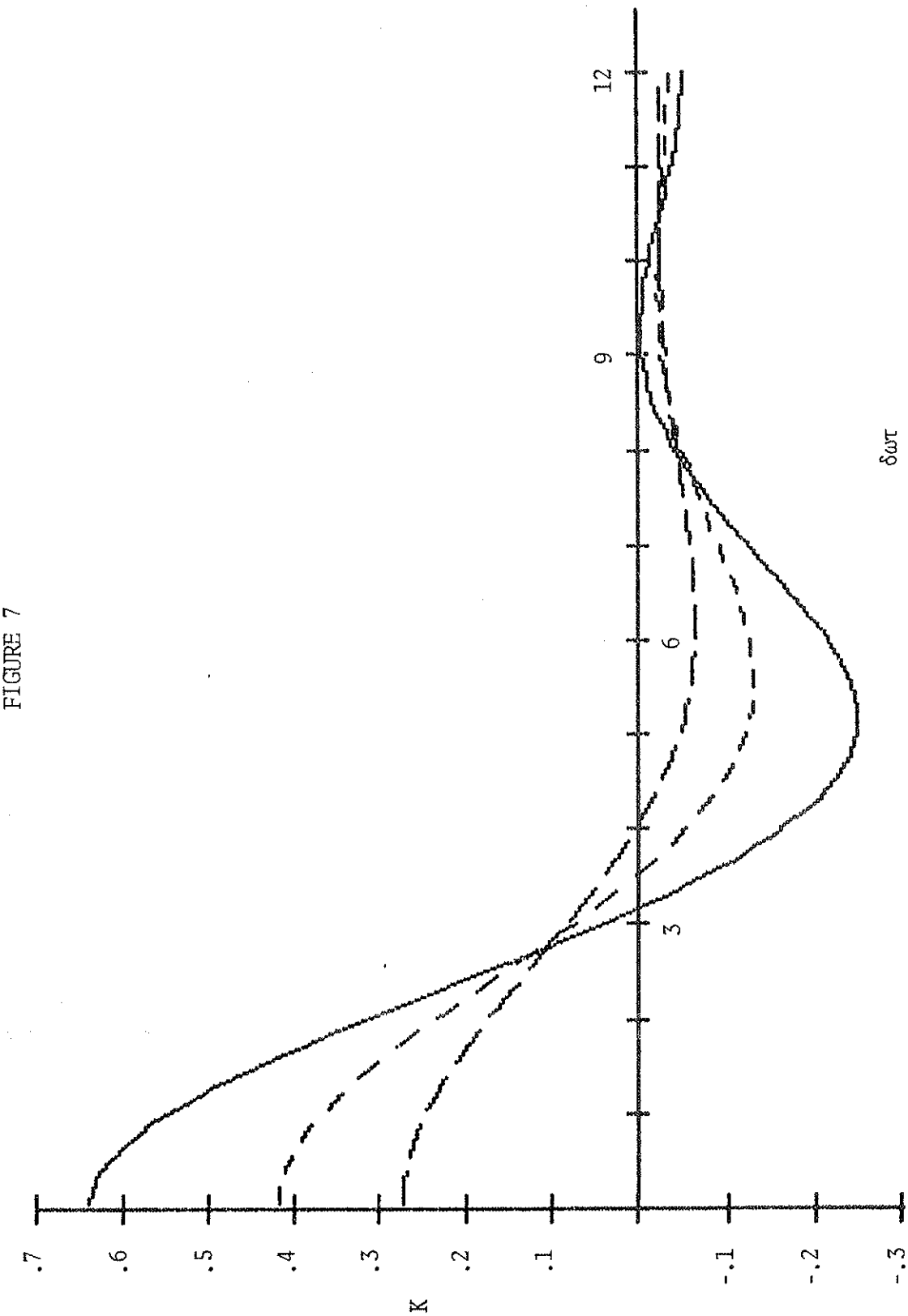

FIGURE 7

Figure 8

The Dispersion Curve for Overdamping and τ Fixed

The function K is displayed vs. $\delta\omega\tau$ for $\tau = 1$, for $\omega' \ll \Gamma$, and for 3 values of Γ :

———— $\Gamma = .1 \quad \omega' = .01$

— — — $\Gamma = 2 \quad \omega' = .1$

—— —— $\Gamma = 4 \quad \omega' = .1$

FIGURE 8

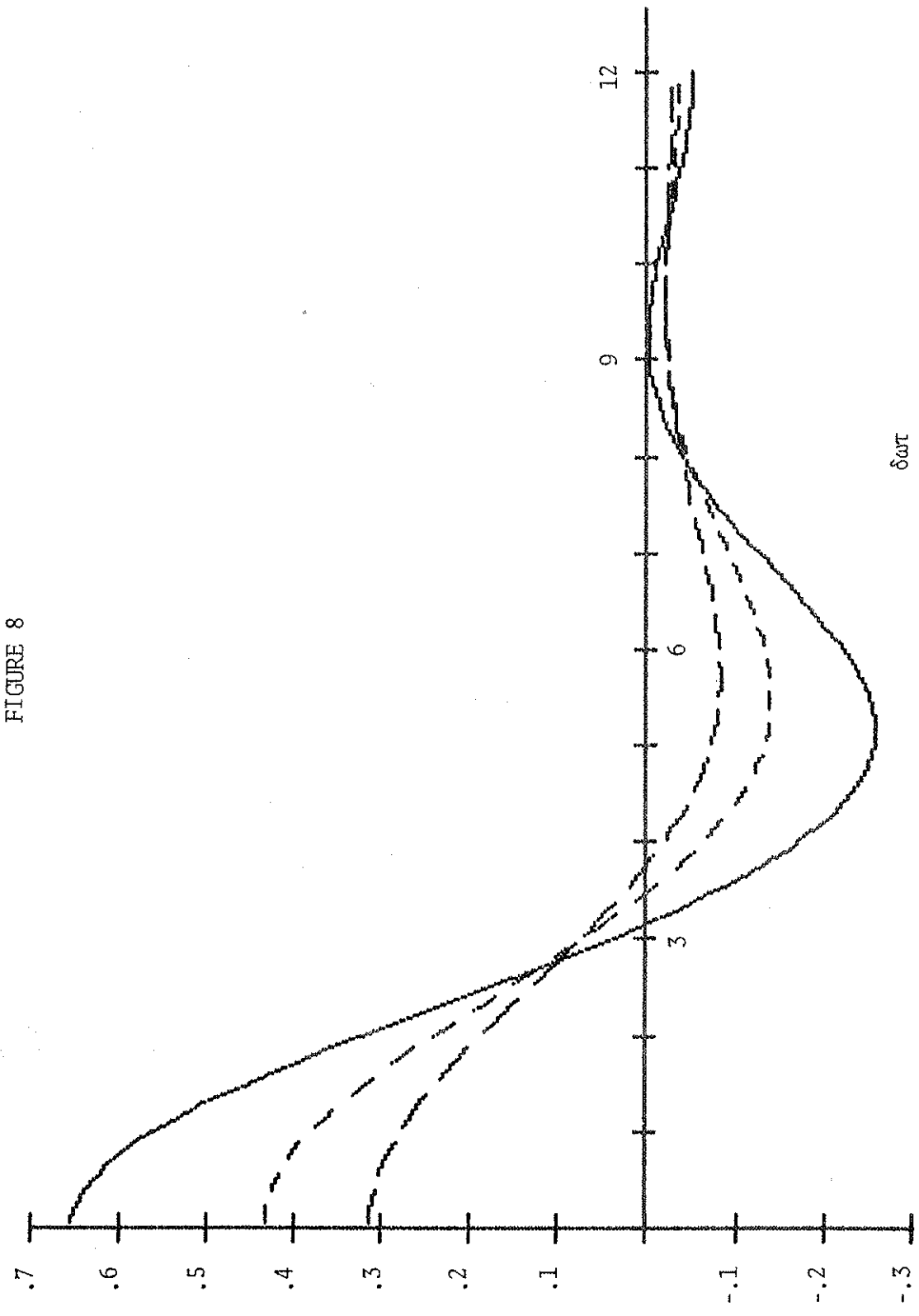

Figure 9

The Gain Curve for Underdamping and $\delta\omega$ Fixed

The function J is displayed vs. $\delta\omega\tau$ for $\delta\omega = 1$, for $\Gamma \ll \omega'$, and for 4 values of ω':

———— $\Gamma = .001 \quad \omega' = .01$

— — — $\Gamma = .01 \quad \omega' = .2$

—— —— $\Gamma = .01 \quad \omega' = .6$

— ——— — $\Gamma = .01 \quad \omega' = .99$

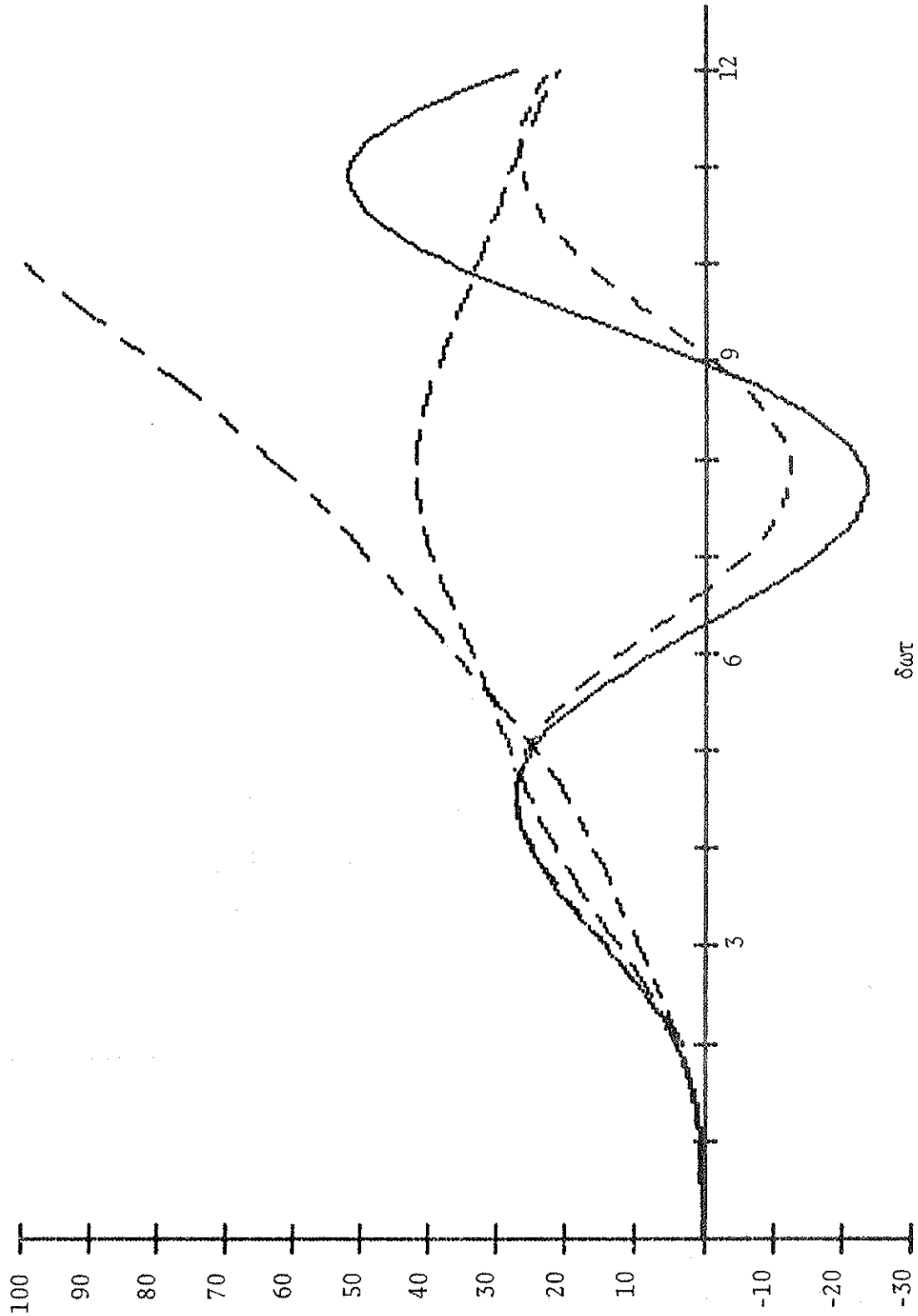

FIGURE 9

Figure 10

The Gain Curve for Critical Damping and $\delta\omega$ Fixed

The function J is displayed vs. $\delta\omega\tau$ for $\delta\omega = 1$, for $\omega' = \frac{1}{2}\Gamma$, and for 3 values of Γ:

———— $\Gamma = .0195$ $\omega' = .01$

— — — $\Gamma = .495$ $\omega' = .25$

—— —— $\Gamma = 1.495$ $\omega' = .75$

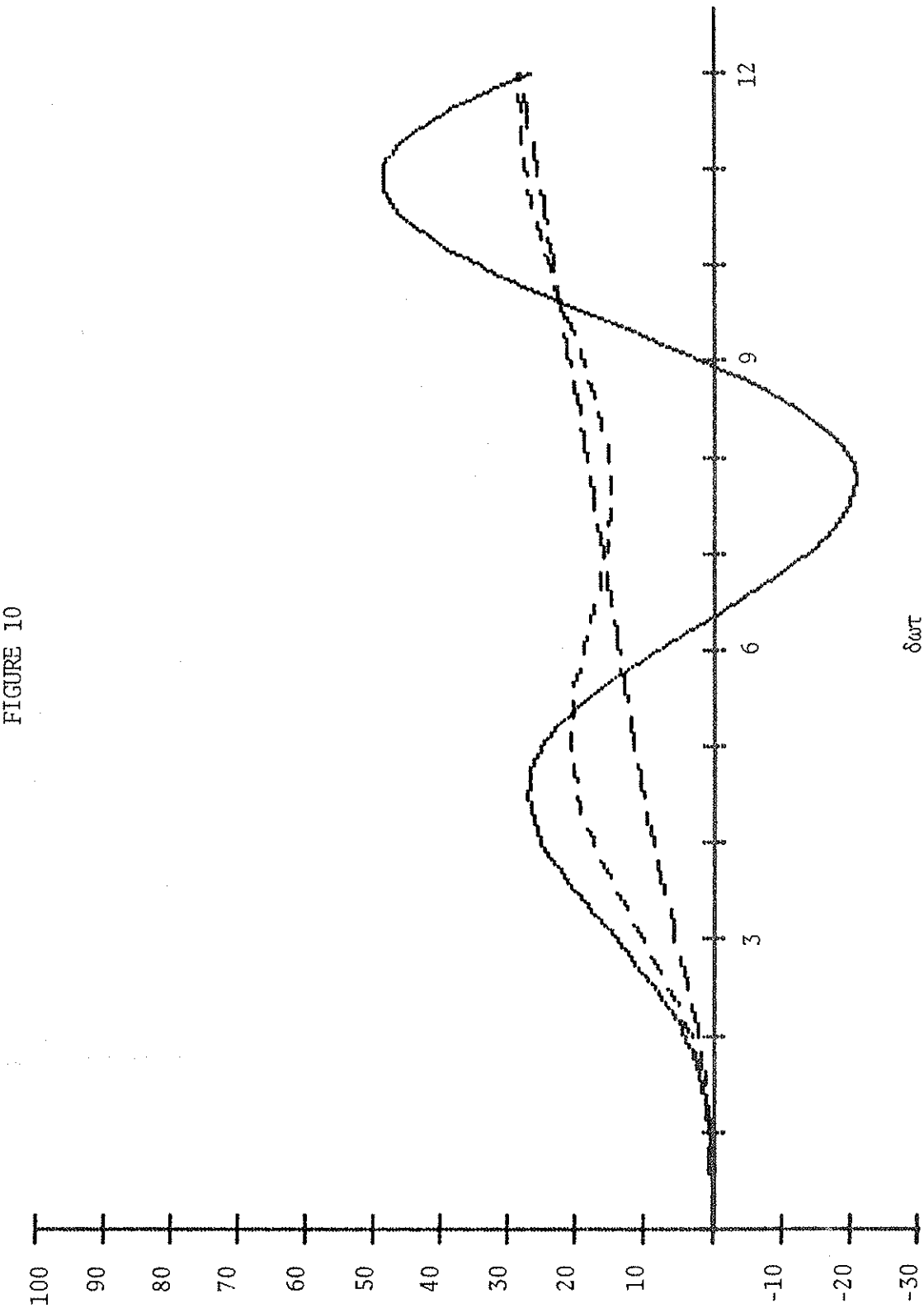

FIGURE 10

Figure 11

The Gain Curve for Overdamping and $\delta\omega$ Fixed

The function J is displayed vs. $\delta\omega\tau$ for $\delta\omega = 1$, for $\omega' \ll \Gamma$, and for 3 values of Γ:

———— $\Gamma = .02 \quad \omega' = .001$

— — — $\Gamma = .5 \quad \omega' = .01$

—— —— $\Gamma = 1.5 \quad \omega' = .01$

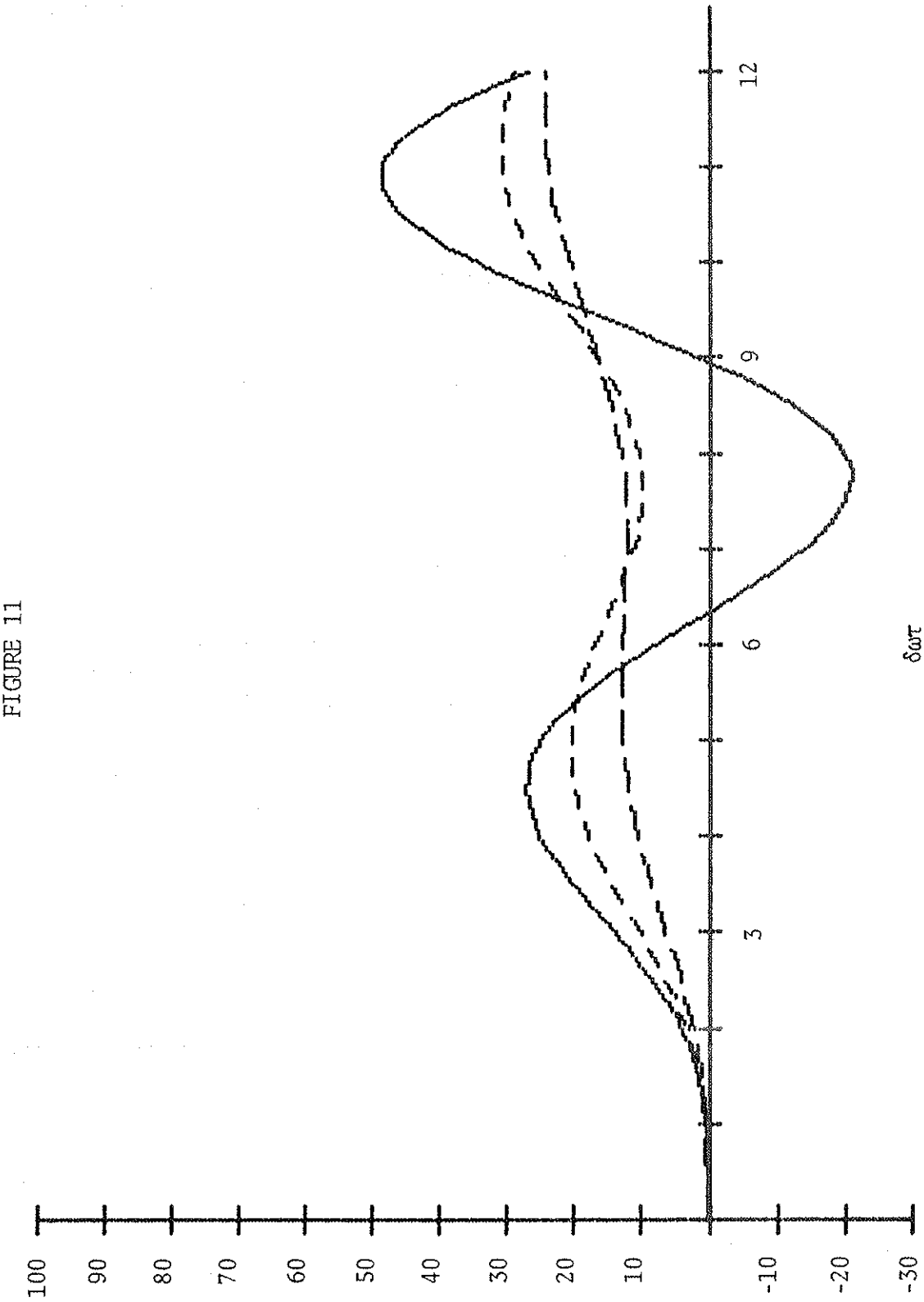

FIGURE 11

Figure 12

The Gain Curve at Resonance With the Plasma Wave

The function J is displayed vs. $\delta\omega\tau$ for $\delta\omega = 1$, for $\tilde{\omega} = \sqrt{\omega'^2 - \frac{1}{4}\Gamma^2} \simeq 1$, and for 3 values of Γ:

———— $\Gamma = .01 \quad \omega' = .99$

— — — $\Gamma = .5 \quad \omega' = 1.03$

—— —— $\Gamma = 1.5 \quad \omega' = 1.24$

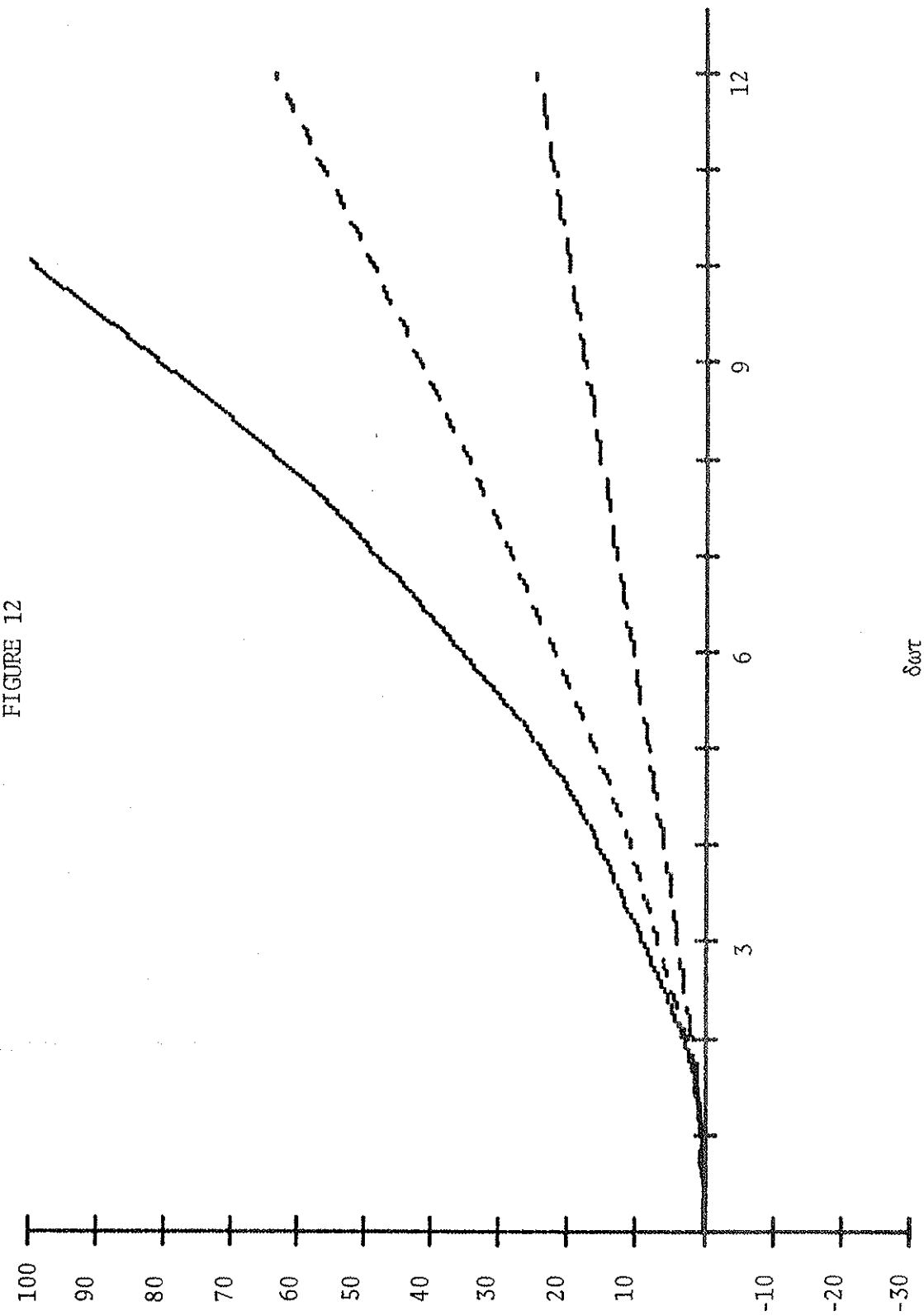

FIGURE 12

Figure 13

The Dispersion Curve for Underdamping and $\delta\omega$ Fixed

The function K is displayed vs. $\delta\omega\tau$ for $\delta\omega = 1$, for $\Gamma \ll \omega'$, and for 4 values of ω':

———— $\Gamma = .001 \quad \omega' = .01$

— — — $\Gamma = .01 \quad \omega' = .2$

—— —— $\Gamma = .01 \quad \omega' = .6$

— ——— — $\Gamma = .00001 \quad \omega' = .999$

FIGURE 13

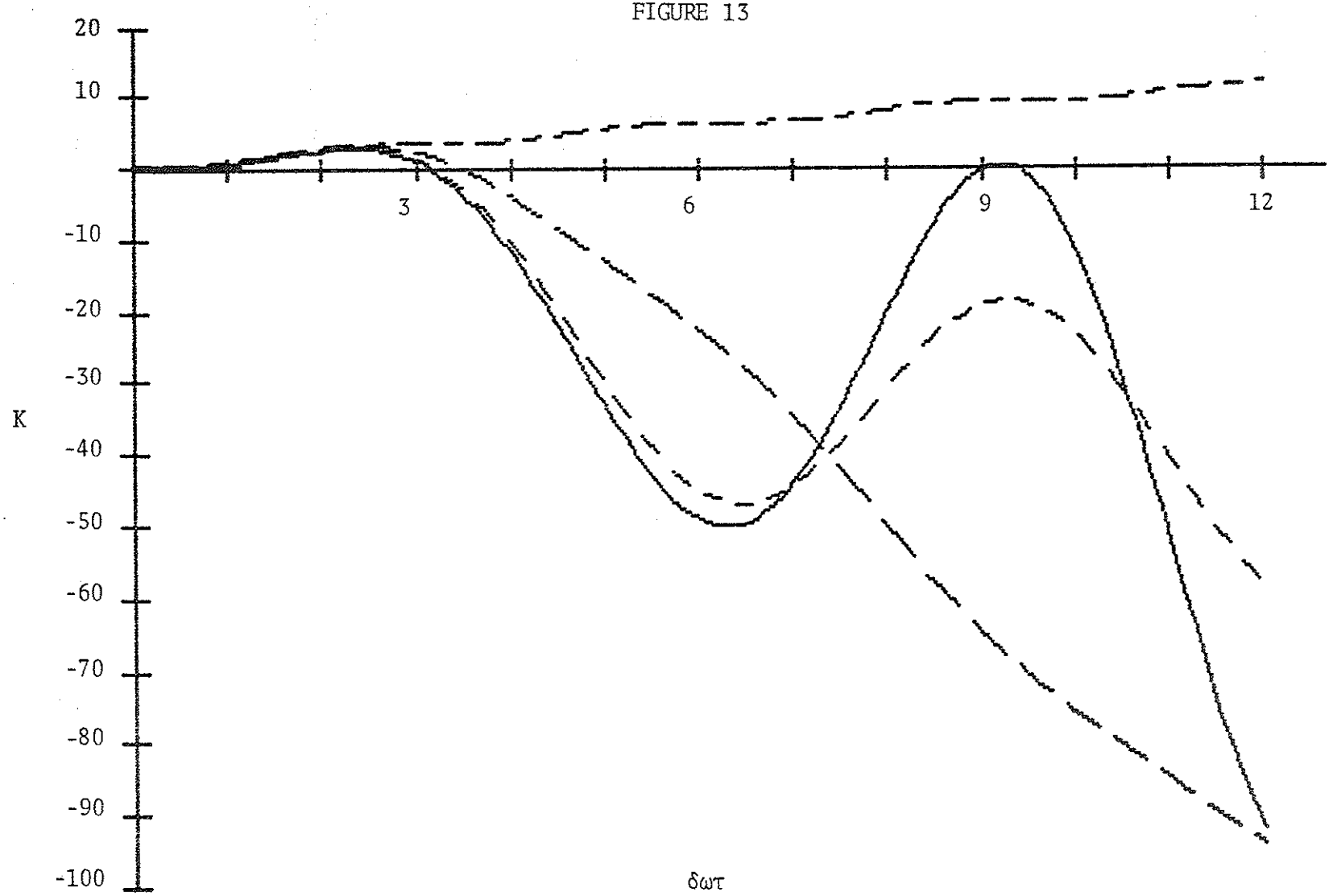

Figure 14

The Dispersion Curve for Critical Damping
and $\delta\omega$ Fixed

The function K is displayed vs. $\delta\omega\tau$ for $\delta\omega = 1$, for $\omega' = \frac{1}{2}\Gamma$, and for 3 values of Γ:

———— $\Gamma = .0195 \quad \omega' = .01$

— — — $\Gamma = .495 \quad \omega' = .25$

—— —— $\Gamma = 1.495 \quad \omega' = .75$

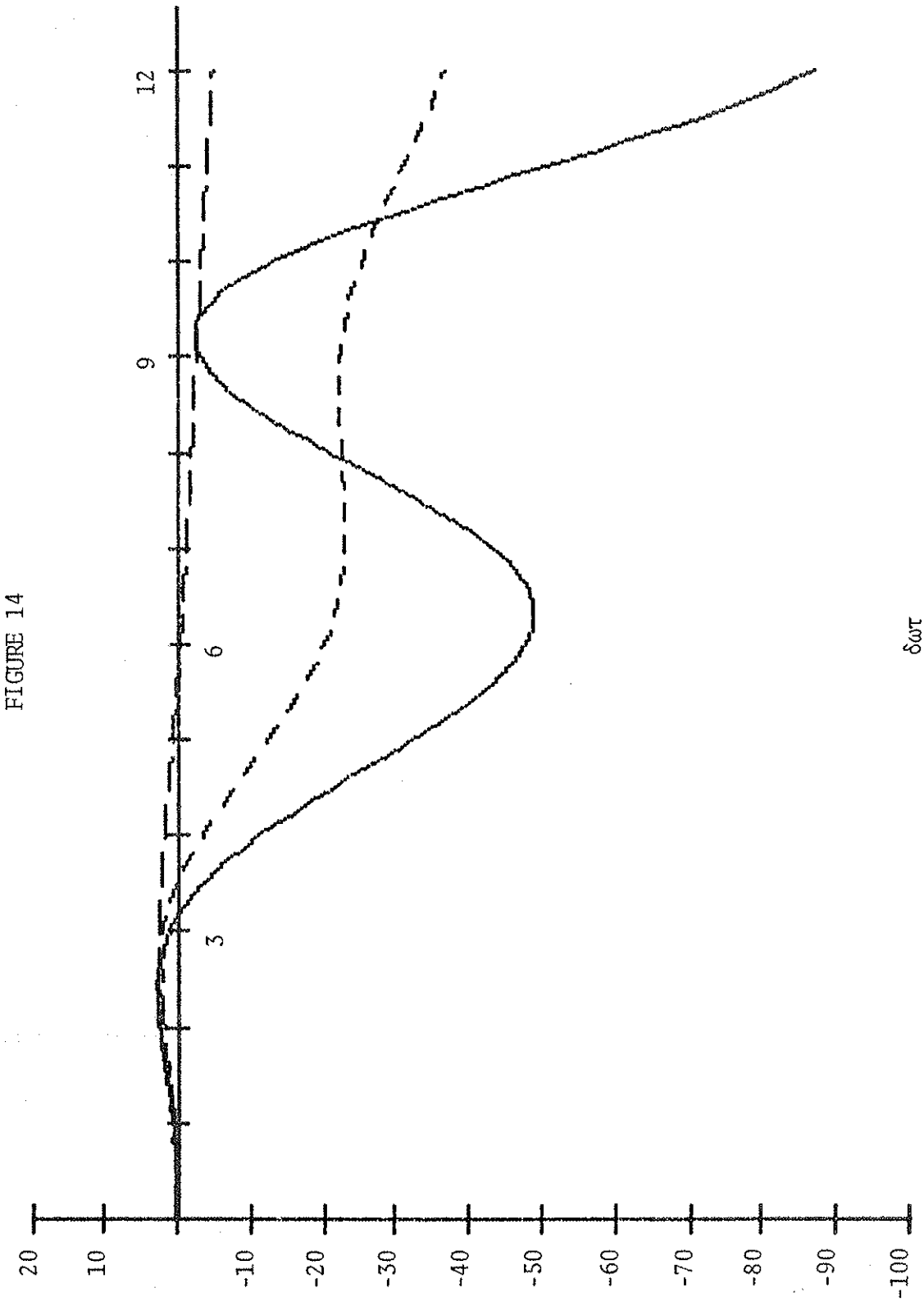

FIGURE 14

Figure 15

The Dispersion Curve for Overdamping and $\delta\omega$ Fixed

The function K is displayed vs. $\delta\omega\tau$ for $\delta\omega = 1$, for $\omega' \ll \Gamma$, and for 3 values of Γ:

———— $\Gamma = .02$ $\omega' = .001$

— — — $\Gamma = .5$ $\omega' = .01$

—— —— $\Gamma = 1.5$ $\omega' = .01$

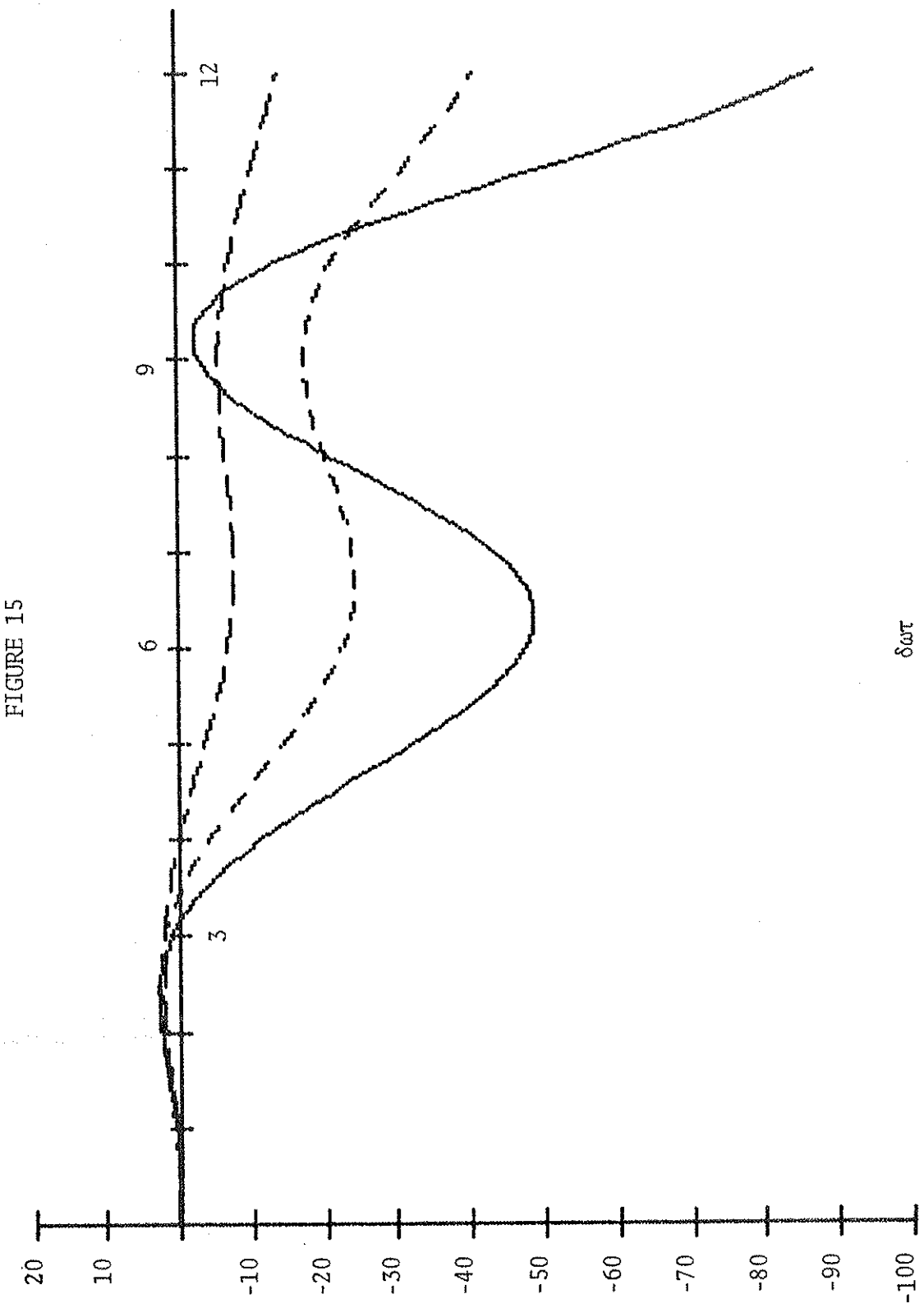

FIGURE 15

Figure 16

The Dispersion Curve at Resonance With the Plasma Wave

The function K is displayed vs. $\delta\omega\tau$ for $\delta\omega = 1$, for $\tilde{\omega} = \sqrt{\omega'^2 - \frac{1}{4}\Gamma^2} \simeq 1$, and for 3 values of Γ:

———— $\Gamma = .00001$ $\omega' = .999$

— — — $\Gamma = .5$ $\omega' = 1.03$

—— —— $\Gamma = 1.5$ $\omega' = 1.249$

FIGURE 16

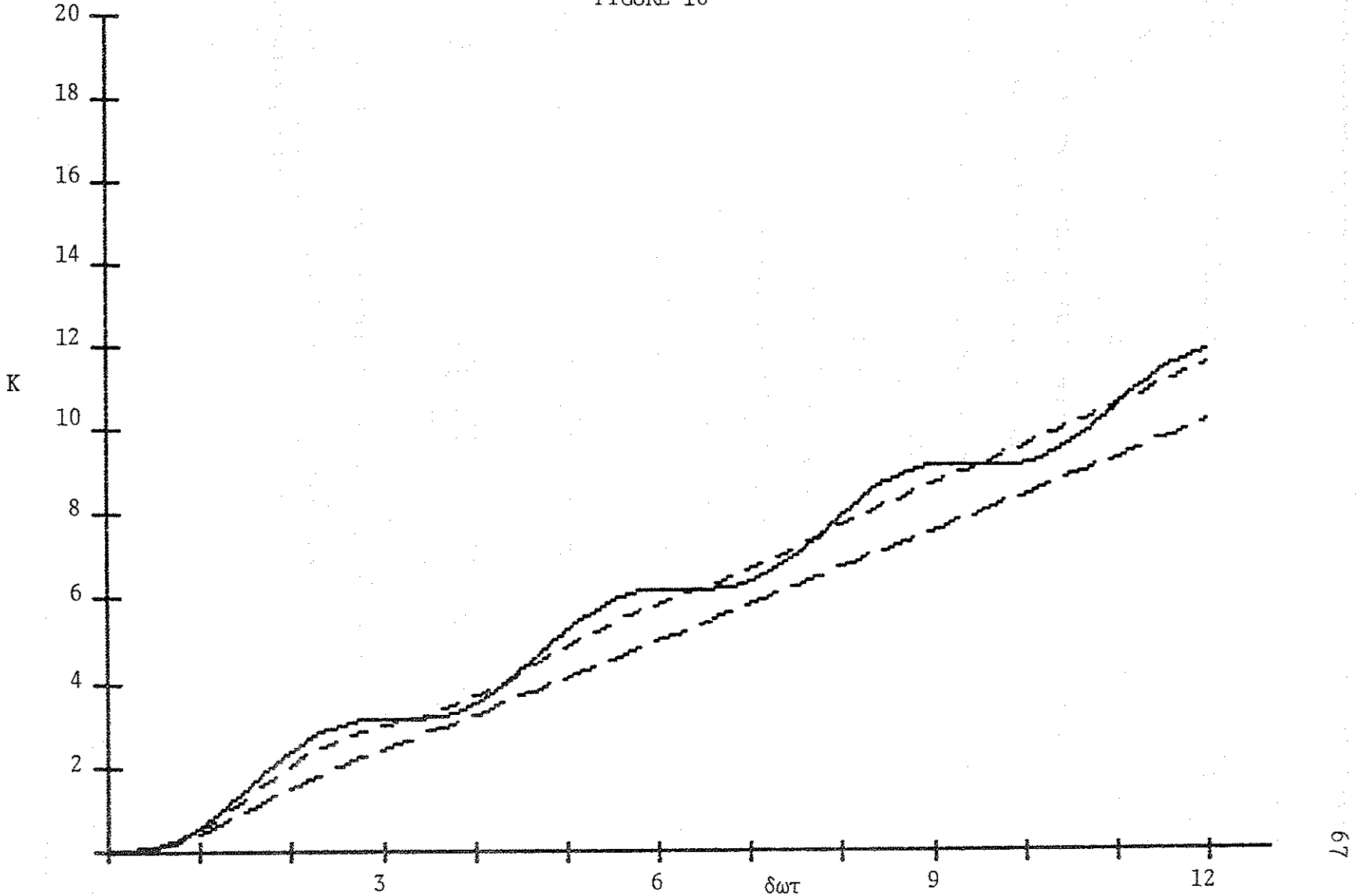

$$\tau^3 L(\delta\omega\tau, \omega'\tau, \Gamma\tau, 1) = L(\delta\omega, \omega', \Gamma, \tau) \qquad (60)$$

where L stands for either J or K.

Figures 9-16 show the functions J and K for case (ii). Of special interest is the change from oscillatory to monotonic behavior as either Γ becomes appreciable, or as resonance with the plasma wave, $\delta\omega = \tilde{\omega} = \sqrt{\omega'^2 - \frac{1}{4}\Gamma^2}$ is approached. The undamped resonant case (see Figs. 9,12,13, and 16) is of special interest since it corresponds to stimulated Raman scattering. For this case, i.e. $\Gamma = 0$ and $\delta\omega = \omega'$, the expressions in Appendix II simplify to

$$J = \frac{\tau^2}{\omega'^2} - \frac{\sin^2\omega'\tau}{\omega'^3} \qquad (61)$$

$$K = \frac{\tau^2}{\omega'^2} - \frac{\sin 2\omega'\tau}{2\omega'^3} \qquad (62)$$

The above expression for K agrees, except for a numerical factor, with an estimate for the frequency shift of the probe wave at resonance given by Schmidt[42]. At resonance, the solution for δn given in Appendix II can also be used to obtain a simple expression for the longitudinal electric field, δE.

$$\delta E = \frac{\pi e c n_o}{\bar{\omega}} \frac{\Omega^2}{\omega'^2} [\ \omega'\tau \cos((k_o+k)z-\omega'\tau) + \cos(k_o+k)z \sin\omega'\tau\ ] \quad (63)$$

The part of the electric field that grows linearly with time agrees with that obtained by Rosenbluth and Liu[37]. Hence, the quadratically increasing transfer of energy from the pump wave to the probe wave is accompanied by a linear increase in the amplitude of the resonant plasma wave. Schmidt[42] also finds the plasma wave to have a linearly growing amplitude. As discussed in Ref. 37, the plasma wave will cease to grow when the particle displacements from equilibrium in the fluid grow to be on the order of the wavelength of the electromagnetic waves. When this large amplitude regime is reached, the plasma wave "breaks" and its energy is rapidly converted to thermal energy through turbulence[65]. Since the particle displacement, δx, and the electrostatic field are related by the expression[37]

$$\delta E = - 4\pi e\, n_o\, \delta x \quad (64)$$

for δx small enough that particle crossing does not occur, setting $\delta x = 1/k$ gives for the time, τ_c, when wave

breaking will limit the energy transfer between the electromagnetic waves,

$$\tau_c \simeq \frac{\omega'}{\Omega^2} \tag{65}$$

Figures 9-16 will not apply for values of τ exceeding this limit. Note that Eq. (60) can be used to find J and K for cases where $\delta\omega \neq 1$.

G. An Approximation to the Inhomogeneously Broadened Limit

It is possible to use these results in the cold fluid limit to obtain an approximation to the gain in the inhomogeneously broadened limit. The kinetic theory of plasma waves predicts that such waves are damped by Landau damping. Indeed, the situation taken here requires the plasma oscillations to have wavelengths in the optical range; for such short wavelengths, the plasma waves are heavily damped. To find the natural frequency corresponding to this short wavelength it is necessary to use the full plasma dispersion function. Once the values of Γ and ω' corresponding to the wavelength $\frac{\lambda}{2\pi} = 1/(k+k_o)$ are found, the correct kinetic treatment of stimulated Thomson scattering can be approximated by using these

values in Eq. (36) and approximating $f(v_z)$ by a superposition of cold fluids with different velocities. In this approximation, the inhomogeneously broadened limit is obtained by folding the general gain curve, Eq. (50), against $f(v_z)$ as was done in Chapter 2. In the limit that $f(v_z)$ is much wider than J, the inhomogeneous gain coefficient is simply proportional to $\int_{-\infty}^{\infty} \eta J(\eta)\, d\eta$. For ω' and Γ very small, this integral has the value $\pi\tau^3$. This integral may also be calculated in the case where ω' and Γ are appreciable by using the more complicated expressions given in Appendix 2. A contour integration shows that the value of the integral for arbitrary Γ, ω', and τ is still $\pi\tau^3$! Hence, in this approximation, Eq. (7) still gives the gain coefficient in the inhomogeneously broadened limit. An inspection of the figures, however, shows that J becomes wider as ω' and Γ become appreciable; it then becomes necessary for the distribution function to be wider to obtain the inhomogeneously broadened limit.

CHAPTER 4

INDEPENDENT ELECTRON THEORY OF STIMULATED THOMSON SCATTERING

A. Gain and Dispersion in the Plasma

In this section sufficient formalism is introduced to determine the gain and dispersion of a plasma, due to stimulated Thomson scattering, in terms of the motion of the electrons in the plasma. As in Chapter 3, two oppositely directed electromagnetic waves, of angular frequencies ω_o and ω, propagating in a plasma are studied. The difference is that here the electric fields produced by the electron motion will be neglected; the motion of the electrons only under the influence of the low frequency ponderomotive force will be examined. Making this simplification allows the saturation of the gain coefficient for stimulated Thomson scattering by non-linear Landau damping to be obtained. The approach taken here is similar to that used by Johnston[60,61], Colson[19], and Cocke[62]. A particularly elegant approach was taken by Bambini and Renieri[63] who used the total hamiltonian, including both fields and particles, to calculate the energy transfer between the two waves.

As in Chapter 3, it is convenient to work in the Coulomb gauge, where $\vec{\nabla}\cdot\vec{A} = 0$, so that the vector potential satisfies the inhomogeneous wave equation,

$$\nabla^2\vec{A} - \frac{1}{c^2}\frac{\partial^2\vec{A}}{\partial t^2} = -\frac{4\pi}{c}\vec{J} + \frac{1}{c}\vec{\nabla}\frac{\partial\Phi}{\partial t} \tag{66}$$

The current density is given by

$$\vec{J} = -e\int d^3r_o\int d^3v_o\ \vec{v}'(\vec{r}_o,\vec{v}_o,t)\delta(\vec{r}-\vec{r}')\ F(\vec{r}_o,\vec{v}_o) \tag{67}$$

The primed coordinates, $\vec{r}'$ and $\vec{v}'$, represent the instantaneous position and velocity at time t of an electron that at time t=0 was at position $\vec{r}_o$ with velocity $\vec{v}_o$. The electron distribution at time t=0 is $F(\vec{r}_o,\vec{v}_o)$, normalized so that its integral over all velocities and over the plasma volume gives the number of electrons in the plasma. The vector potential is assumed to be of the form given in Eq. (10).

The procedure used in Eqs. (41)-(42) of Chapter 3 is also used here to obtain the following equation for $\dot{\theta}$.

$$\dot{\theta} = \frac{4\pi\omega}{EV\,t\,ck} \int_0^t dt^* \int_V d^3\vec{r}\, \cos(kz+\omega t^*)\, \hat{x}\cdot\vec{J} \qquad (68)$$

Equation (67) is now used to convert the right hand side of Eq. (68) into a time integral along particle orbits, averaged over initial positions and velocities. Since ω and ω_o are assumed to be well above the plasma frequency, so that $\frac{\omega}{ck} \simeq 1$, Eq. (68) can be written in the form

$$\dot{\theta} = -\frac{4\pi e}{VEt} \int_V d^3\vec{r}_o \int d^3\vec{v}_o \int_0^t dt^*\, \cos(kz'+\omega t^*) v_x' F(\vec{r}_o, \vec{v}_o) \qquad (69)$$

Eq. (68) can be given a simple physical interpretation by writing it in the form

$$(2\dot{\theta})\, \frac{E^2}{8\pi} = \frac{1}{Vt} \int_V d^3\vec{r} \int_0^t dt^*\, \vec{E}\cdot\vec{J} \qquad (70)$$

where $E = -E\cos(kz+\omega t)\,\hat{x}$. The left hand side of Eq. (70) is the product of $2\dot{\theta}$ and the energy density, U, of the probe wave. The right hand side of Eq. (70) is the average of $\vec{E}\cdot\vec{J}$ for the probe wave. Hence, Eq. (70) can be written in the form

$$\frac{d}{dt}(U) = \frac{1}{Vt}\int_V d^3r_o \int_0^t dt^* \; E \cdot J \qquad (71)$$

as expected.

The same procedure used in Chapter 3 is also used here to obtain an equation for $\frac{1}{2}(\omega - k^2c^2/\omega) + \dot{\phi}$.

$$\tfrac{1}{2}\left(\omega - \frac{k^2c^2}{\omega}\right) + \dot{\phi}$$

$$= -\frac{4}{VEt}\int_V d^3\vec{r} \int_0^t dt^* \; \sin(kz+\omega t)\; \hat{x}\cdot\vec{J} \qquad (72)$$

Eq. (67) is now used to convert the right hand side of Eq. (72) into a time integral along particle orbits, averaged over initial positions and velocities.

$$\tfrac{1}{2}\left(\omega - \frac{k^2c^2}{\omega}\right) + \dot{\phi}$$

$$= \frac{4\pi e}{VEt}\int_V d^3\vec{r}_o \int d^3\vec{v}_o \int_0^t dt^* \; \sin(kz'+\omega t^*)\, v_x' F(\vec{r}_o, \vec{v}_o) \qquad (73)$$

Useful expressions for $\dot{\theta}$ and $\dot{\phi}$ can be obtained if the details of the electron motion are known; this is the subject of the next section.

Henceforth the prime notation is dropped on quantities to be evaluated at the position of the

electron. It will be understood that integrals of the type in Eq. (69) are to be taken along electron orbits.

B. Particle Orbits

In this section the orbits of plasma electrons under the influence of the two electromagnetic waves are calculated. It is assumed that θ, ϕ, θ_o, and ϕ_o are so small that the wave fields may be taken to be constant over the plasma volume. The scalar potential, Φ , is neglected in solving for the particle orbits. Comparison of the electrostatic term and the ponderomotive term in Eq. (35) shows that electrostatic effects are negligible if $\omega_p << \delta\omega$.

The Lagrangian for an electron with these approximations is

$$L = \frac{1}{2}mv^2 - \frac{e}{c}\vec{v}\cdot\vec{A} = \frac{1}{2}m\,(v_x^2 + v_y^2 + v_z^2) - \frac{v_x e}{c}\left[\frac{E_o c}{\omega_o}\sin(k_o z-\omega_o t) + \frac{Ec}{\omega}\sin(kz+\omega t)\right] \quad (74)$$

Since x and y are ignorable coordinates, there are two constants of the motion,

$$p_x = mv_x - \frac{e}{c}\left[\frac{E_o c}{\omega_o}\sin(k_o z-\omega_o t) + \frac{Ec}{\omega}\sin(kz+\omega t)\right] \quad (75)$$

and

$$p_y = m\, v_y \quad (76)$$

Lagrange's equation for z yields

$$m\,\dot{v}_z + \frac{e}{c}\left[\frac{E_o c k_o}{\omega_o}\cos(k_o z - \omega_o t) + \frac{Eck}{\omega}\cos(kz+\omega t)\right] v_x = 0 \quad (77)$$

Combining Eqs. (75) and (77) yields

$$\begin{aligned} m\,\dot{v}_z = &-\frac{ep_x}{mc}\left[E_o\cos(k_o+\omega_o t) + E\cos(kz+\omega t)\right] \\ &-\frac{e^2}{mc}\left[\frac{E_o^2}{2\omega_o}\sin(2k_o z-2\omega_o t) + \frac{E^2}{2\omega}\sin(2kz+2\omega t)\right. \\ &+\frac{E_o E}{\omega}\cos(k_o z-\omega_o t)\sin(kz+\omega t) \\ &\left.+\frac{E_o E}{\omega_o}\sin(k_o z-\omega_o t)\cos(kz+\omega t)\right] \end{aligned} \quad (78)$$

The first four terms on the right hand side of Eq. (78) represent forces that oscillate at optical frequencies.

Assuming electron temperatures of a few kilovolts, or less, and laser intensities of about 10^{13} W/cm^2, these terms contribute z-displacements far less than the wavelength of either electromagnetic wave. The first four terms are therefore neglected. As in Chapter 3, the last two terms on the right hand side of Eq. (78) are combined to yield a low frequency ponderomotive force,

$$F_p = - \frac{e^2 E_o E}{mc\bar{\omega}} \sin((k_o+k)z - \delta\omega t) \qquad (79)$$

where $\bar{\omega} = \frac{1}{2}(\omega_o+\omega)$ and $\delta\omega = \omega_o - \omega$. This term is the classical recoil force that causes stimulated Thomson scattering; the oscillation of a particle produced by the electric field of one wave combines with the magnetic field of the other wave to produce a force in the z-direction. This low frequency force can contribute displacements comparable to the wavelengths of the two electromagnetic waves for $\delta\omega \leq 10^{-3}\,\bar{\omega}$. This low frequency approximation to Eq. (78) yields

$$\frac{d^2 z}{dt^2} = - \frac{e^2 E_o E}{m^2 c\bar{\omega}} \sin((k_o+k)z - \delta\omega t) \qquad (80)$$

The physical significance of this equation can be seen by making a Galilean transformation to a frame of reference where the two waves are Doppler shifted so that they have the same frequency:

$$\tilde{z} = z - \left(\frac{\delta\omega}{k_o+k} \right) t \tag{81}$$

In the $\tilde{z}$ coordinate system, Eq. (80) becomes

$$\frac{d^2}{dt^2}\tilde{z} = - \frac{e^2 E_o E}{m^2 c \bar{\omega}} \sin(k_o+k)\tilde{z} \tag{82}$$

Equation (82) shows that in this frame the particles move in a time independent potential. Particles with small $\tilde{z}$ velocities are trapped in the minima of this potential and execute harmonic motion. Particles with $\tilde{z}$ velocities on the order of $\tilde{v}_z = \sqrt{4e^2 E_o E/(m^2 \bar{\omega}\, c(k_o+k)}$ are "barely trapped" in the potential minima and tend to "stick" near the peaks of the potential. Particles with $\tilde{z}$ velocities well above $\tilde{v}_z$ are not trapped; the potential only causes a slight ripple in their $\tilde{z}$ velocities.

It is convenient to make the change of variable

$$\xi = (k_o+k)\tilde{z} = (k_o+k)z - \delta\omega t \qquad (83)$$

so that Eq. (80) becomes the simple pendulum equation

$$\frac{d^2}{dt^2}\,\xi = -\Omega^2 \sin\xi \qquad (84)$$

where $$\Omega^2 = \frac{(k_o+k)e^2E_oE}{m^2c\,\bar{\omega}} \simeq \frac{2E_oEe^2}{m^2c^2}$$

The swinging, "sticking," and rotating solutions of the simple pendulum equation correspond, respectively, to trapped, "barely trapped," and untrapped particles in the reference frame described by Eq. (81). The solutions of the simple pendulum equation are given in terms of Jacobian Elliptic Functions. These functions arise naturally when discussing particle motion in sinusoidal waves, and have been used to estimate the non-linear Landau damping of electrostatic waves[66,67]. Milne-Thomson's notation for these functions is used[68]. To describe the solutions, two quantities, ε and p, are defined by the equations

$$\varepsilon^2 = \dot{\xi}^2 + 4\,\Omega^2 \sin^2 \frac{\xi}{2} \tag{85}$$

and

$$p = \left(\frac{\varepsilon}{2\Omega} \right)^2 \tag{86}$$

Note that ε is a constant of the motion, analogous to the energy of a pendulum. The two types of solutions of Eq. (84) are now described.

(1) Swinging Solutions

These solutions are characterized by the condition $0 \leq p \leq 1$, and satisfy the equation

$$\sin \frac{\xi}{2} = \frac{\varepsilon}{2\Omega} \, \mathrm{sn}[\Omega(t-t_o) \mid p] \tag{87}$$

From Eq. (87) it follows that

$$\dot{\xi} = \varepsilon \, \mathrm{cn}[\Omega(t-t_o) \mid p] \tag{88}$$

making it useful to define a reduced distribution function by the equation

$$f(v_{zo}) = \frac{1}{n_e} \int_{-\infty}^{\infty} dv_{xo} \int_{-\infty}^{\infty} dv_{yo}\ F(\vec{r}_o, \vec{v}_o) \tag{95}$$

where $\int_{-\infty}^{\infty} f(v_{zo})\ dv_{zo} = 1$.

The expression for v_x' obtained from Eq. (75) is substituted into Eq. (69). In the resulting expression, all terms with frequencies on the order of $\overline{\omega}$ nearly time average to zero; they are neglected. If a cylindrical plasma volume of area A in the x-y plane and length L in the z-direction is used, Eq. (69) becomes

$$\dot{\theta} = -\frac{2\pi e^2 n_e E_o}{E\ m\ \omega_o\ L} \int_{-\infty}^{\infty} dv_{zo} \int_{-L/2}^{L/2} d_{zo}\ f(v_{zo}) \quad X \quad \sin(\ (k_o+k)z - \delta\omega t\ ) \tag{96}$$

The variables are now changed from z', z_o, and v_{zo} to ξ, ξ_o , and $\dot{\xi}_o$ according to the equations

$$\xi = (k_o+k)z - \delta\omega t \tag{97}$$

$$\xi_o = (k_o+k)z \tag{98}$$

and

$$\dot{\xi}_o = (k_o+k)\, v_{zo} - \delta\omega \tag{99}$$

Using Eq. (84) to perform the time integration yields

$$\theta = \frac{2\pi e^2 n_e E_o}{LEm\ \omega_o (k_o+k)^2 \Omega^2} \quad X$$

$$\int_{-\infty}^{\infty} d\dot{\xi}_o \int_{-(k_o+k)L/2}^{(k_o+k)L/2} d\xi_o [\dot{\xi}(\tau) - \dot{\xi}_o] f\left(\frac{\xi_o+\delta\omega}{k_o+k}\right) \tag{100}$$

The integrand is periodic in ξ_o with period 2π; ignoring end effects, Eq. (100) becomes

$$\theta = \frac{e^2\ n_e\ E_o}{Em\omega_o (k_o+k)\Omega^2} \int_{-\infty}^{\infty} d\dot{\xi}_o \int_{-\pi}^{\pi} d\xi_o [\dot{\xi}(\tau) - \dot{\xi}_o]\ f\left(\frac{\xi_o+\delta\omega}{k_o+k}\right) \tag{101}$$

This is the general expression for θ. A similar calculation yields θ_o. The relationship between θ and θ_o was discussed in Chapter 3 (see Eq. (54)).

In the homogeneously broadened limit, Doppler broadening is unimportant; this limit is obtained by setting

$$f\left(\frac{\xi_o+\delta\omega}{k_o+k}\right) = (k_o+k)\,\delta(\dot{\xi}_o+\delta\omega) \qquad (102)$$

Using this distribution function, Eq. (101) becomes

$$\theta = \frac{4\pi^2 n_e r_e^2 I_o c}{m\,\omega_o} J \qquad (103)$$

where

$$J(\delta\omega\tau,\Omega\tau) = \frac{4}{\pi\Omega^4}\int_{-\pi}^{\pi} d\xi_o\,[\,\dot{\xi}(\tau) + \delta\omega\,] \qquad (104)$$

and

$$I_o = \frac{c}{8\pi} E_o^2 \qquad (105)$$

For general values of $\delta\omega\tau$ and $\Omega\tau$, J is difficult to evaluate analytically. In the limit that $\beta = (\frac{2\Omega}{\delta\omega})^2 << 1$ and $\Omega\tau \leq 1$, however, it is possible to obtain an approximate expression for J by expanding the integrand of Eq. (104) in powers of β.

Note that in this limit, only rotating solutions are used, so that Eq. (104) can be written as

$$J = \frac{4}{\pi\Omega^4} \int_{\pi}^{\pi} d\xi_o \left[\varepsilon \, dn\left(\varepsilon(t-t_o)/2 \mid (\frac{2\Omega}{\varepsilon})^2 \right) + \delta\omega \right] \quad (106)$$

where

$$\varepsilon = - \left[\delta\omega^2 + 4\Omega^2 \sin^2 \frac{\xi_o}{2} \right]^{\frac{1}{2}} \quad (107)$$

and

$$\sin \frac{\xi_o}{2} = sn\left[- \frac{\varepsilon t_o}{2} \mid (\frac{2\Omega}{\varepsilon})^2 \right] \quad (108)$$

The expansion of the integrand of Eq. (106) is tedious, but straightforward; Useful identities are given in Appendix 4. To second order in β, J is given by the equation

$$J = \tau^3 \frac{d}{d\eta} \left(\frac{\sin^2\eta}{\eta^2} \right) \quad (109)$$

in agreement with Eq. (52). As stated, the expansion for J is valid when $\Omega\tau \leq 1$ and when $\beta << 1$. This implies that $\eta >> \Omega\tau$. Equation (109) is also valid

FIGURE 17

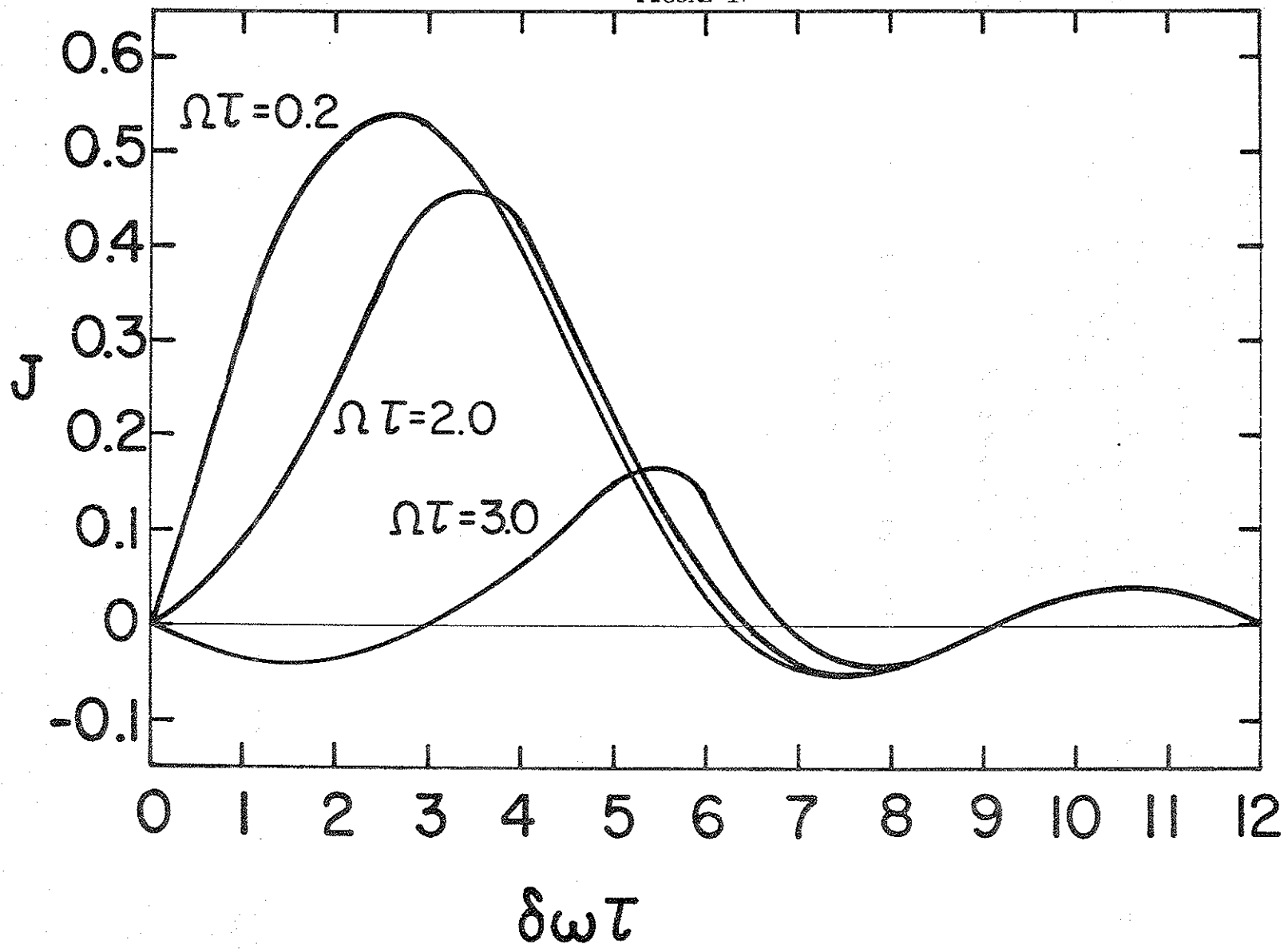

Figure 18

The Saturation of the Homogeneously Broadened Gain Curve vs. $\Omega\tau$

The function J is displayed vs. $\Omega\tau$ for $\tau = 1$ and for 4 values of $\delta\omega\tau$.

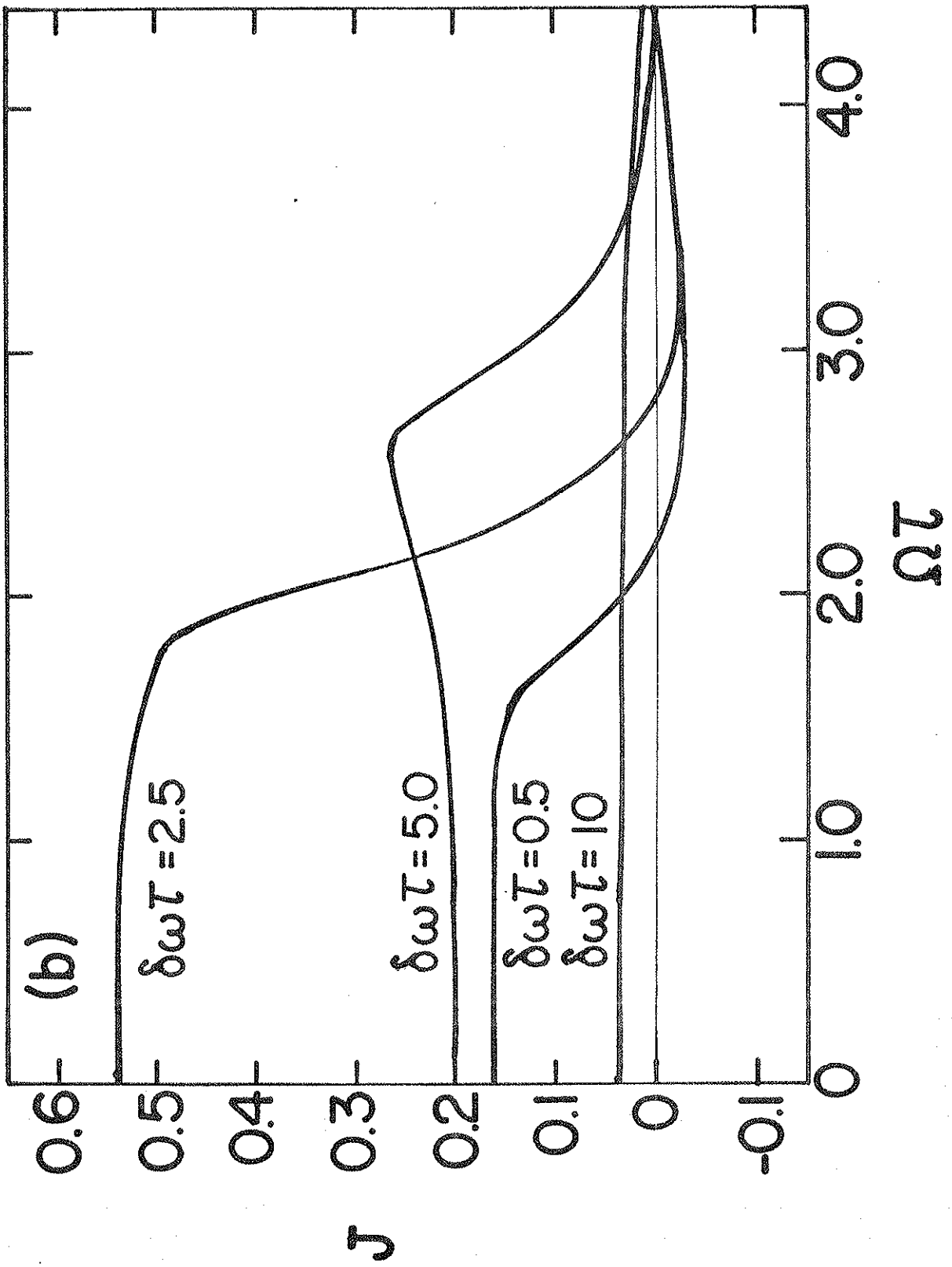

FIGURE 18

D. The Phase Shift, ϕ, in the Homogeneously Broadened Limit

In this section ϕ is calculated using the same assumptions about the distribution function and the plasma volume given in Section C. The expression for v_x' obtained from Eq. (75) is substituted into Eq. (73). In the resulting expression, the high frequency terms are time averaged, the variables z', z_o, and v_{xo} are changed to ξ, ξ_o, and $\dot{\xi}_o$, and the equation is integrated over the interaction time, τ. Equating terms of like order yields Eq. (44) again and an expression for ϕ.

$$\phi = - \frac{e^2 n_e E_o}{m\omega_o E(k_o+k)} \int_{-\infty}^{\infty} d\dot{\xi}_o \int_{-\pi}^{\pi} d\xi_o \cos \xi \, f\left(\frac{\dot{\xi}_o+\delta\omega}{k_o+k}\right) \qquad (111)$$

This is the general expression for ϕ.

In the homogeneously broadened limit, Eq. (102) is used to obtain

$$\phi = - \frac{4\pi^2 n_e r_e^2 I_o c}{m \omega_o} K \qquad (112)$$

where

$$K(\delta\omega\tau,\Omega\tau) = \frac{4}{\pi\Omega^2}\int_0^{\tau} dt \int_{-\pi}^{\pi} d\xi_o \cos\xi \qquad (113)$$

In the limit that $\beta << 1$ and $\Omega\tau \leq 1$, K is given by

$$K = \frac{4}{\pi\Omega^4}\int_0^{\tau} dt \int_{-\pi}^{\pi} d\xi_o \left[1 - 2\, sn^2(\varepsilon(t-t_o)/2 \,|\, (\frac{2\Omega}{\varepsilon})^2)\right] \qquad (114)$$

To first order in β,

$$K = \tau^3 \frac{d}{d\eta}\left(\frac{1}{\eta} - \frac{\sin 2\eta}{2\eta^2}\right) \qquad (115)$$

for $\eta >> \Omega\tau$. This expression is also valid for $\eta \leq \Omega\tau$ if $\Omega\tau << 1$. Hence, in the unsaturated limit ($\Omega\tau << 1$)

$$\phi = -\frac{4\pi^2 n_e r_e^2 I_o c \tau^3}{m \omega_o} \frac{d}{d\eta}\left(\frac{1}{\eta} - \frac{\sin 2}{2\eta^2}\right) \qquad (116)$$

Equation (58) may be used to interpret $\dot{\phi}$ as a non-linear part of the index of refraction.

If β is no longer small, ϕ must be calculated numerically. Figure 19 shows K as a function of $\delta\omega\tau$

Figure 19

The Saturation of the Homogeneously Broadened Dispersion Curve vs. $\delta\omega\tau$

The function K is displayed vs. $\delta\omega\tau$ for $\tau = 1$ and for 3 values of $\Omega\tau$.

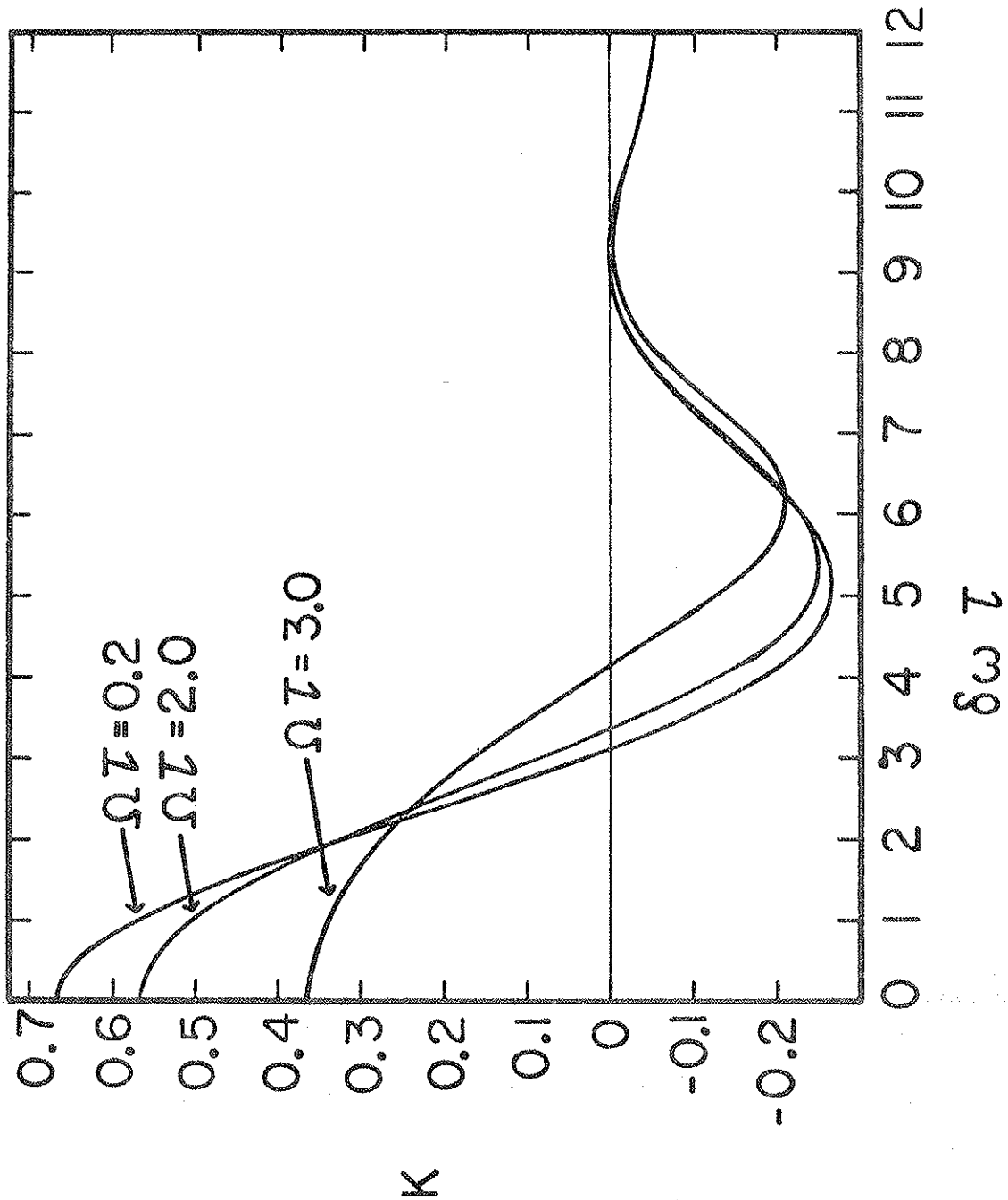

FIGURE 19

Figure 20

The Saturation of the Homogeneously Broadened Dispersion Curve vs. $\Omega\tau$

The function K is displayed vs. $\Omega\tau$ for $\tau = 1$ and for 4 values of $\delta\omega\tau$.

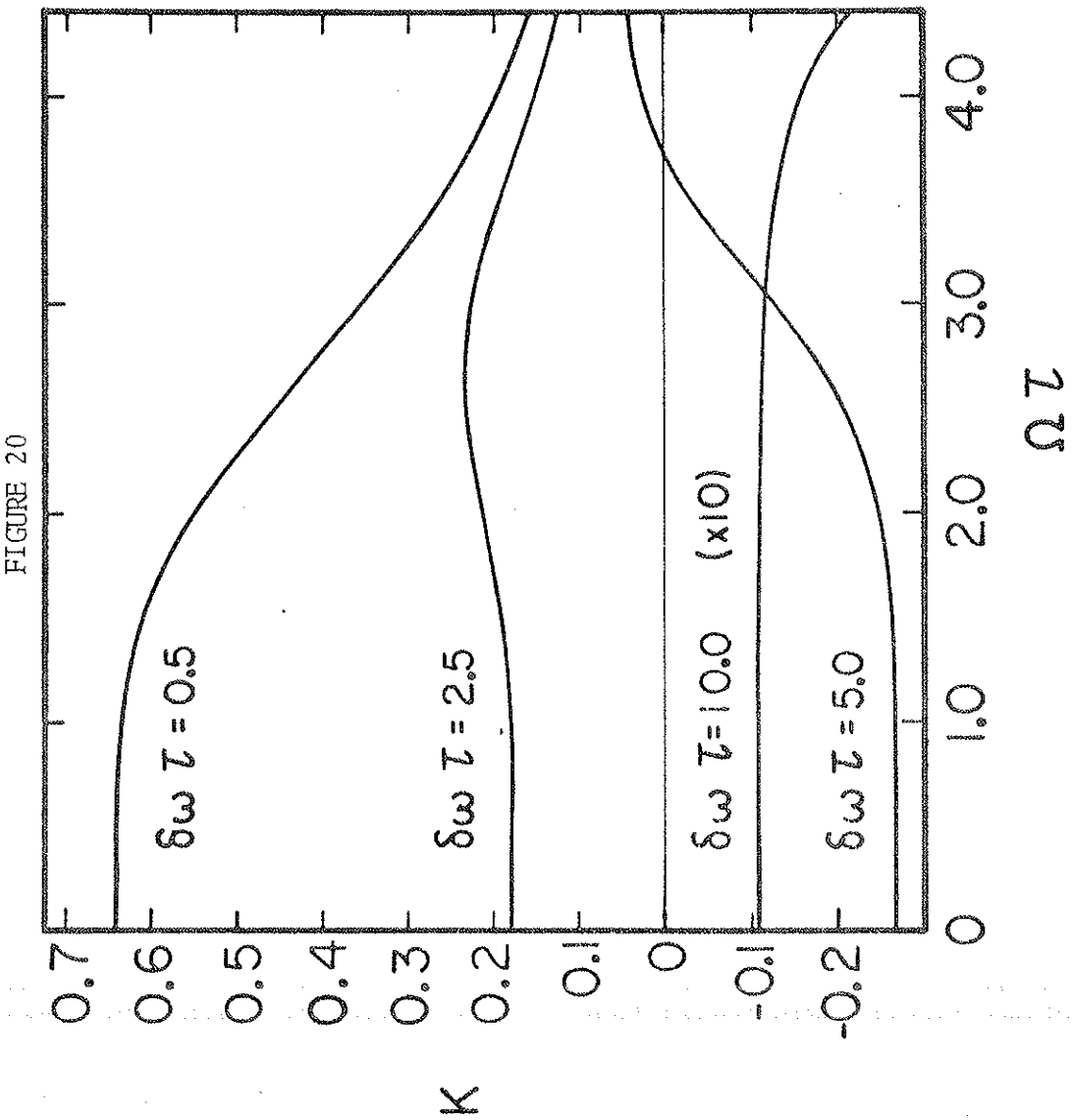
0.7
0.6
0.5
0.4
0.3
0.2
0.1
0
-0.1
-0.2
K
0
1.0
2.0
3.0
4.0
Ω τ
δω τ = 0.5
δω τ = 2.5
δω τ = 10.0 (x10)
δω τ = 5.0

FIGURE 20

for selected values of $\Omega\tau$ and for $\tau = 1$. Figure 20 shows K as a function of $\Omega\tau$ for selected values of $\delta\omega\tau$ and for $\tau = 1$. Note that like the homogeneous gain, the homogeneous dispersion saturates more easily near $\eta = 0$ than in the wings of the lineshape.

E. The Gain and the Phase Shift in the Inhomogeneously Broadened Limit

When the electrons in a plasma have a distribution of velocities, the gain can be obtained as a simple convolution of the homogeneous gain formula with the electron distribution function. Equation (101), Eq. (103), and the expression for the distribution function,

$$f\left(\frac{\dot{\xi}_o+\delta\omega}{k_o+k}\right) = \int_{-\infty}^{\infty} d\sigma\ \delta(\sigma-\dot{\xi}_o-\delta\omega)\ f\left(\frac{\sigma}{k_o+k}\right) \qquad (117)$$

can be combined to yield the equation

$$\theta = \frac{4\pi^2 r_e^2 n_e I_o c}{m\ \omega_o (k_o+k)} \int_{-\infty}^{\infty} d\sigma\ f\left(\frac{\sigma}{k_o+k}\right)\ J((\delta\omega-\sigma)\tau, \Omega\tau) \qquad (118)$$

In the unsaturated limit, Eq. (109) gives the expression for J; substituting it into Eq. (118) and integrating by parts yields

$$\theta = \frac{16\pi^2 r_e^2 n_e I_o c\tau}{m\,\omega_o (k_o+k)^2} \int_{-\infty}^{\infty} d\lambda\; f'\left[\frac{1}{k_o+k}(\delta\omega+2\lambda/\tau)\right]\frac{\sin^2\lambda}{\lambda^2} \qquad (119)$$

where $\lambda = (\sigma - \delta\omega)\,\tau/2$. In the inhomogeneous limit, the width, in λ, of the distribution function is much larger than the width of the homogeneous gain curve. This limit is described by the condition

$$\frac{\overline{v_z}}{c} \gg \frac{1}{\omega\tau} \qquad (120)$$

where $\overline{v_z}$ is the width, in velocity, of the distribution function $f(v_z)$. In this limit, the slope of the electron distribution function is nearly constant over the width of the homogeneous gain curve. Setting $f'[(\delta\omega + 2\lambda/\tau)/(k_o+k)] \simeq f'\left[\frac{\delta\omega}{k_o+k}\right]$ in the integrand of Eq. (119) and using the result that $\int_{-\infty}^{\infty}\sin^2\lambda/\lambda^2 = \pi$, yields for the inhomogeneously broadened gain in the unsaturated limit

$$\gamma\tau = 2\theta = -\frac{8\pi^3 r_e^2 n_e I_o c^3 \tau}{m\,\omega_o^3} \left.\frac{df}{dz}\right|_{v_z=\frac{(\omega_o-\omega)c}{2\omega_o}} \qquad (121)$$

in agreement with the quantum mechanical result, Eq. (7).

If the gain is allowed to saturate, then the homogeneous gain curve is no longer given by Eq. (109). The saturated homogeneous gain curve is flattened near the center, but is still an odd function of $\delta\omega\tau$, as shown in Figure 18. A function M is defined by the equation

$$M(\lambda,\Omega\tau) = \int_{\infty}^{\lambda} J(-2\lambda',\Omega\tau)\, d\lambda' \qquad (122)$$

Equation (118) is integrated by parts to obtain an equation for the saturated inhomogeneous gain coefficient:

$$\gamma\tau = - \frac{32\pi^2 r_e^2 n_e I_o c\tau}{m\omega_o (k_o+k)^2} \int_{-\infty}^{\infty} d\lambda \; f'[(\delta\omega+2\lambda/\tau)/(k_o+k)]M \quad (123)$$

If the distribution function is much wider than M, Eq. (123) may be written as

$$\gamma\tau = - \frac{8\pi^3 r_e^2 n_e I_o c^3 \tau}{m\ \omega_o^3} \quad \Delta(\Omega\tau) \quad \left.\frac{df}{dz}\right|_{v_z=\frac{(\omega_o-\omega)c}{2\omega_o}} \quad (124)$$

where

$$\Delta(\Omega\tau) = \int_{-\infty}^{\infty} M(\lambda,\Omega\tau)d\lambda = \int_{-\infty}^{\infty} \lambda\ J(-2\lambda,\Omega\tau)d\lambda \quad (125)$$

The quantity $\Delta(\Omega\tau)$ is shown in Figure 21.

The expression for ϕ, Eq. (111), can also be expressed, in the inhomogeneously broadened limit, as a convolution of the homogeneous expression, Eq. (112), with the distribution function:

Figure 21

The Saturation of the Inhomogeneously Broadened Gain

The function Δ is displayed vs. $\Omega\tau$.

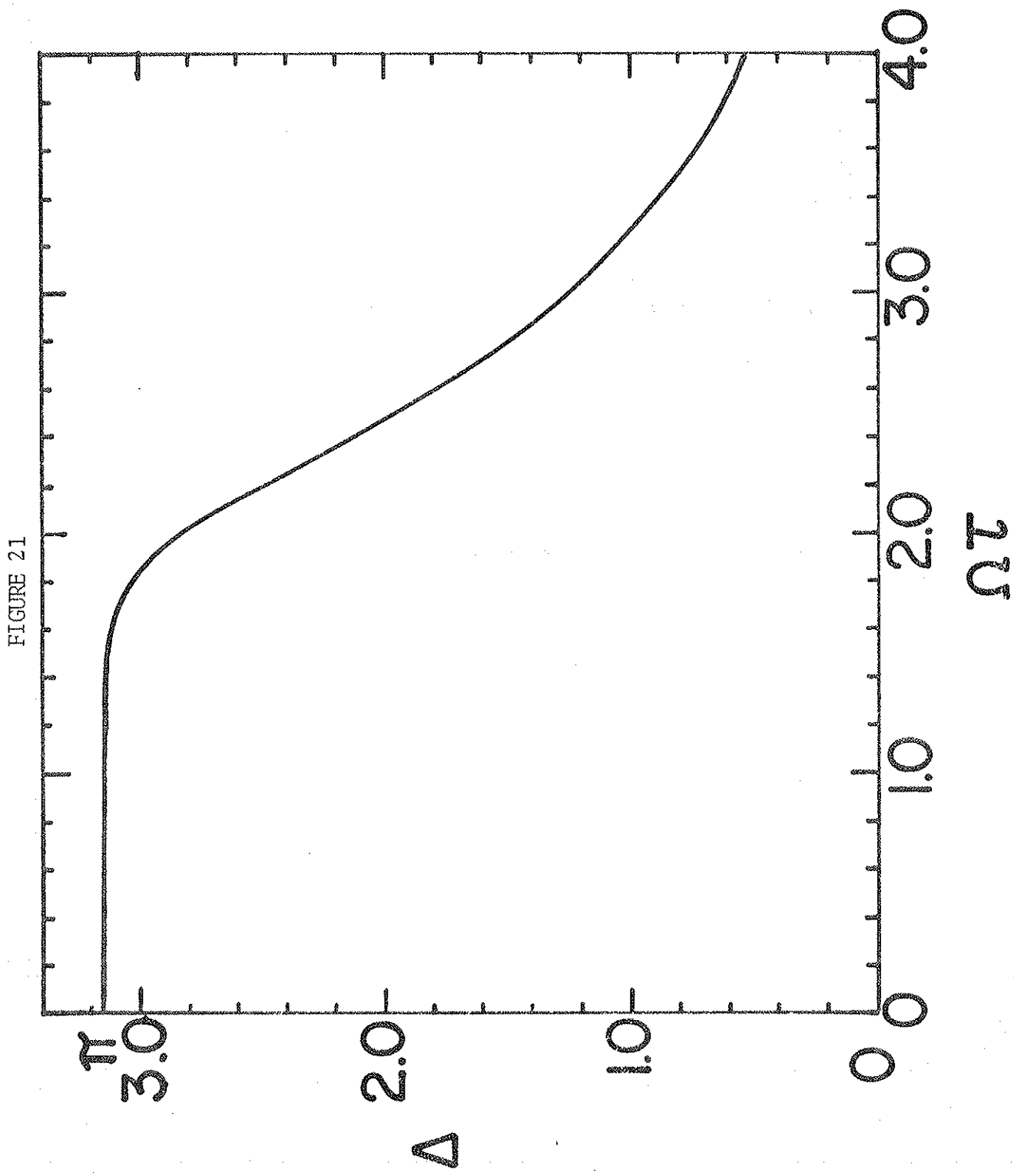

FIGURE 21

$$\phi = - \frac{4\pi^2 r_e^2 n_e I_o c}{m\omega_o(k_o+k)} \int_{-\infty}^{\infty} f\left(\frac{\sigma}{k_o+k}\right) K((\delta\omega-\sigma)\tau, \Omega\tau)\, d\sigma \qquad (126)$$

In the unsaturated limit, Eq. (109) is used to obtain the equation

$$\phi = \frac{16\pi^2 r_e^2 n_e I_o c\tau^2}{m\omega_o(k_o+k)} \frac{d}{d(\delta\omega)} \int_{-\infty}^{\infty} f\left(\frac{\sigma}{k_o+k}\right) \chi \left[\frac{1}{(\sigma-\delta\omega)\tau} - \frac{\sin(\sigma-\delta\omega)\tau}{(\sigma-\delta\omega)^2\tau^2} \right] d\sigma \qquad (127)$$

In the inhomogeneous limit, the distribution function is nearly constant, in σ, over the center of K. Since this curve is odd, the center of K makes only a small contribution to ϕ. There is, however, a significant contribution from the wings of K; in fact, since the integral of $1/(\sigma - \delta\omega)\tau$ diverges at large σ, it samples the entire width of the distribution function. It is convenient to replace the fairly complicated function K by a simpler function that also contributes nothing for σ near $\delta\omega$, and that has the same behavior for $|\sigma| >> \delta\omega$. Such a function is $P\frac{1}{(\sigma-\delta\omega)\tau}$, where P stands for principal value. In this approximation, Eq. (127) becomes

$$\phi = \frac{8\pi^2 r_e^2 n_e I_o c^2 \tau}{m\,\bar{\omega}^2} \frac{d}{d(\delta\omega)} \left[P \int_{-\infty}^{\infty} d\sigma \frac{f(\frac{\sigma}{k_o + k})}{\sigma - \delta\omega} \right] \qquad (128)$$

If the distribution function is Maxwellian,

$$f(v_z) = \sqrt{\frac{m}{2\pi k_B T}}\, e^{-mv_z^2/2k_B T} \qquad (129)$$

then Eq. (128) becomes

$$\phi = \frac{4\pi^2 r_e^2 n_e I_o c^3 \tau}{k_B T\, \bar{\omega}^3} Z'(y) \qquad (130)$$

where y is given by Eq. (9) and where

$$Z'(y) = \frac{d}{dy}\left[\mathrm{Re}\left(\frac{1}{\sqrt{\pi}} P \int_{-\infty}^{\infty} dx \frac{e^{-x^2}}{x - y} \right) \right] \qquad (131)$$

is the derivative of the real part of the plasma dispersion function for a real argument[69]. For the case of a Maxwellian distribution function, the ratio of the correct expression, Eq.(127), to the approximate expression, Eq. (130), can, for y = 0, be shown to be $1 - \mathrm{erf}(N)/N$, where $N = (2k_B T/mc^2)^{\frac{1}{2}}\, \omega\tau$. Hence, for

$N \geq 20$, Eq. (130) is good to 10% or better at line center.

If ϕ is allowed to saturate, then K changes near $\delta\omega = 0$, but remains nearly the same as in the unsaturated limit for $\delta\omega >> 1/\tau$. Figure 19 shows that for $\delta\omega \gtrsim \Omega$, the saturated K and the unsaturated K are nearly the same. From Eq. (126), saturation in the inhomogeneously broadened phase shift should only become important when $2\Omega \gtrsim (k_o+k)v_{th}$, or when $\Omega \gtrsim v_{th}\omega/c$. The inhomogeneous gain, on the other hand, saturates when $\Omega\tau \sim 1$. Since $v_{th}\,\omega/c >> 1$ in most cases, the inhomogeneous gain will usually saturate much more easily than the inhomogeneously broadened phase shift.

It is interesting to note that the way the folding together of the distribution function with the homogeneously broadened lineshape, $\frac{d}{d\eta}(\sin^2\eta/\eta^2)$, gives rise to the first derivative of the distribution function in the inhomogeneously broadened limit, Eq. (108), is analogous to the way the first derivative of the distribution function appears in the Landau damping formula. In the physical derivation of Landau damping given by Dawson[70], the same function, $\frac{d}{dx}(\sin^2x/x^2)$, appears in exactly the same way. Indeed, the unsaturated gain due to stimulated Thomson scattering arises from a process analogous to linear Landau damping while the

saturation mechanism discussed in Sections C-E of this chapter is analogous to non-linear Landau damping.

CHAPTER 5

SUMMARY

The process of stimulated Thomson scattering can thus be thought of in three ways. Firstly, it can be viewed quantum mechanically as the result of photons obeying Bose-Einstein statistics. Secondly, it can be viewed as the result of the transient response of an electron fluid to the ponderomotive beat force between two counterpropagating electromagnetic waves when the frequency difference between the two waves is far above the plasma frequency. As the difference frequency is allowed to approach the plasma frequency, stimulated Thomson scattering passes continuously into stimulated Raman scattering. Thirdly, it can be viewed as the result of a resonant particle interaction. Thought of in this way, the decrease in the gain coefficient as $\delta\omega\tau$ is increased to values much greater than one is due to the phase velocity of the ponderomotive beat wave becoming so large that the electrons are no longer close to resonance. Pursuing the resonant particle picture leads to the observation of non-linear Landau damping of the effect. This damping arises because different electrons have different phases with respect to the beat wave when

$$\sqrt{2}\,\Omega\tau = \left[\frac{16\pi\, r_e^2\, B^2\, I^*}{m^2 c}\right]^{\frac{1}{4}} \frac{L}{\gamma c} \qquad (1.5)$$

(vi) If n^* is the electron density in the laboratory, then the electron density in the electron frame is given by the equation

$$n = \frac{n^*}{\gamma} \qquad (1.6)$$

(vii) If $q = 2\pi/\lambda_q$, then the homogeneous line shape variable, η, is given by the equation

$$\eta = -\frac{\delta\omega\tau}{2} = \frac{L}{2}\left(\frac{\omega^*}{2\gamma^2 c} - q\right) \qquad (1.7)$$

The gain per pass of the amplifier in the electron frame can be calculated by noting that in the electron frame, two pulses appear to be passing through each other. The pump wave pulse is much shorter than the probe wave pulse. Each part of the probe wave pulse sees the interaction last for a time $\tau/2$, but during that interaction time it encounters electrons with interaction times ranging from 0 to τ, linearly distributed in time.

Hence, the total gain of each part of the probe wave pulse, ignoring end effects, is given by the equation

$$G = 2 \int_0^{\tau/2} [2\dot{\theta}(2t)]\, dt = 2\,\theta(\tau) \qquad (1.8)$$

Since this is just the ratio of the final intensity to the initial intensity, Eq. (1.8) also gives the gain per pass in the laboratory. Hence, the small signal gain coefficient per unit length of the magnet in the laboratory, α^*, is given by the equation

$$\alpha^* = \frac{G}{L} = \frac{r_e^2\, n^*\, B^2\, \lambda_q\, L^2\, F}{2\, mc^2\, \gamma^3} \left(\frac{J}{\tau^3}\right) \qquad (1.9)$$

where F is a filling factor that gives the fraction of the electromagnetic wave cross-section that interacts with the electron beam (assuming that the wave cross-section is larger than the beam cross section). In the unsaturated limit, Eq. (109) may be used to write Eq. (1.9) as

$$\alpha^* = \left(\frac{3}{2} n^* \sigma_T\right)\left(\frac{B^2}{8\pi mc^2}\right)\left(\frac{\lambda_q L^2}{\gamma^3} F\right)\frac{d}{d\eta}\left(\frac{\sin^2\eta}{\eta^2}\right) \qquad (1.10)$$

in agreement with the results obtained by others[9,13,19,21].

In evaluating Eq. (1.10) for the free electron amplifier, care must be taken in evaluating γ; it is reduced from its value when the electrons are outside of the helical field since the electrons spiral down the helix. The factor γ is given by the equation

$$\gamma = \frac{E}{mc^2\left[1 + \left(\lambda_q^2 r_e B^2\right)/\left(4\pi^2 mc^2\right)\right]^{\frac{1}{2}}} \qquad (1.11)$$

where E is the electron energy.

When the parameters of the free electron amplifier experiment are used to calculate the peak gain per pass, G, from Eq. (1.10), it is found to be 5.4%. The experiment measured a peak gain per pass of 7%. When the same parameters are used to calculate the saturation parameter, $\sqrt{2}\,\Omega\tau$, it is found to be 2.7. Figures 17 and 21 show that this value is just past threshold for saturation; the theory presented in this thesis predicts that for $I^* = 1.4 \times 10^5 W/cm^2$, the highest power level

attained in the free electron amplifier experiment, the gain is near saturation. No saturation was observed in the experiment. I believe that any significant increase in the value of the laser intensity in the free electron amplifier above the maximum value used will produce saturation effects in the gain. Others have discussed other mechanisms by which the free electron amplifier may saturate[8,16,19,21].

APPENDIX 2

THE PERTURBED DENSITY AND THE FUNCTIONS J AND K FOR GENERAL Γ AND ω'

In this appendix the general solution of Eq. (36) and the resulting expressions for θ and ϕ are given. When Γ and ω' are non-zero, the solution of Eq. (36) subject to the initial conditions given in Eqs. (38) and (39) is

$$\delta n = \frac{-n_o \Omega^2}{\left[(\delta\omega^2 - \tilde{\omega}^2 - \tfrac{1}{4}\Gamma^2)^2 + \Gamma^2\delta\omega^2 \right]} \; X$$

$$\{ (\delta\omega^2 - \tilde{\omega}^2 - \tfrac{1}{4}\Gamma^2)\cos((k_o+k)z - \delta\omega t) + \Gamma\delta\omega \sin((k_o+k)z - \delta\omega t)$$

$$+ e^{-\Gamma t/2} \left[- (\delta\omega^2 - \tilde{\omega}^2 - \tfrac{1}{4}\Gamma^2) \cos(k_o+k)z \cos\tilde{\omega}t \right. \qquad (2.1)$$

$$- \frac{\delta\omega}{\tilde{\omega}} (\delta\omega^2 - \tilde{\omega}^2 + \tfrac{1}{4}\Gamma^2) \sin(k_o+k)z \sin\tilde{\omega}t$$

$$- \Gamma\delta\omega \sin(k_o+k)z \cos\tilde{\omega}t$$

$$\left. + \frac{\Gamma}{2\tilde{\omega}} (\delta\omega^2 + \tilde{\omega}^2 + \tfrac{1}{4}\Gamma^2) \cos(k_o+k)z \sin\tilde{\omega}t \right] \}$$

where $\tilde{\omega} = \sqrt{\omega'^2 - \tfrac{1}{4}\Gamma^2}$

To find $\dot{\theta}$ and $\dot{\phi}$, it is necessary to time and space average the non-linear current, $\frac{4\pi}{c} e \delta n \vec{v}_o$, against either

$\cos(kz)\cos(\omega t)$ or $\cos(kz)\sin(\omega t)$ as was done in the simple case discussed in Chapter 3. If the symbol $< >$ is defined by

$$<f> = \frac{1}{Lt}\int_{-L/2}^{L/2} dz \int_0^t dt' f \qquad (2.2)$$

where it is assumed that $1/\omega << t << 1/\delta\omega$ and that $L >> 1/(k-k_o)$, then $\dot{\theta}$ and $\dot{\phi}$ are given by the equations

$$-\frac{E}{2c}\dot{\theta} = \frac{4\pi e}{c} < \delta n\, v_{ox} \cos kz \cos\omega t' > \qquad (2.3)$$

$$\frac{E}{2c}\dot{\phi} = \frac{4\pi e}{c} < \delta n\, v_{ox} \cos kz \sin\omega t' > \qquad (2.4)$$

Carrying out the operation on the right hand sides of both equations allows them to be written in the same form as Eqs. (45) and (46).

$$\dot{\theta} = \frac{4\pi^2 n_o r_e^2 I_o c}{m \bar{\omega}} P \qquad (2.5)$$

$$\dot{\phi} = -\frac{4\pi^2 n_o r_e^2 I_o c}{m \bar{\omega}} Q \qquad (2.6)$$

where P and Q are now given by the expressions

$$P = \frac{4}{[\,(\delta\omega^2 - \tilde{\omega}^2 - \tfrac{1}{4}\Gamma^2)^2 + \Gamma^2\delta\omega^2\,]} \{\ \Gamma\delta\omega +$$

$$e^{-\Gamma t/2} [\ (\delta\omega^2 - \tilde{\omega}^2 - \tfrac{1}{4}\Gamma^2) \cos\tilde{\omega}t \sin\delta\omega t$$

$$- \frac{\delta\omega}{\tilde{\omega}} (\delta\omega^2 - \tilde{\omega}^2 + \tfrac{1}{4}\Gamma^2) \sin\tilde{\omega}t \cos\delta\omega t - \Gamma\delta\omega \cos\tilde{\omega}t \cos\delta\omega t \qquad (2.7)$$

$$- \frac{\Gamma}{2\tilde{\omega}} (\delta\omega^2 + \tilde{\omega}^2 + \tfrac{1}{4}\Gamma^2) \sin\tilde{\omega}t \sin\delta\omega t\ ]\ \}$$

$$Q = \frac{4}{[\,(\delta\omega^2 - \tilde{\omega}^2 - \tfrac{1}{4}\Gamma^2)^2 + \Gamma^2\delta\omega^2\,]} \{\ -(\delta\omega^2 - \tilde{\omega}^2 - \tfrac{1}{4}\Gamma^2) +$$

$$e^{-\Gamma t/2} [\ (\delta\omega^2 - \tilde{\omega}^2 - \tfrac{1}{4}\Gamma^2) \cos\tilde{\omega}t \cos\delta\omega t$$

$$+ \frac{\delta\omega}{\tilde{\omega}} (\delta\omega^2 - \tilde{\omega}^2 + \tfrac{1}{4}\Gamma^2) \sin\tilde{\omega}t \sin\delta\omega t + \Gamma\delta\omega \cos\tilde{\omega}t \sin\delta\omega t \qquad (2.8)$$

$$- \frac{\Gamma}{2\tilde{\omega}} (\delta\omega^2 + \tilde{\omega}^2 + \tfrac{1}{4}\Gamma^2) \sin\tilde{\omega}t \cos\delta\omega t\ ]\ \}$$

The functions P and Q can be integrated to obtain the generalizations of the functions J and K defined in

the simple case of Chapter 3 by Eqs. (52) and (53). Two separate cases must be considered, (i) underdamping of the plasma wave where $\omega' \geq \frac{1}{2}\Gamma$, and (ii) overdamping where $\omega' < \frac{1}{2}\Gamma$. For case (i) integration of Eqs. (2.7) and (2.8) yields

$$J = \frac{4}{[\,(\delta\omega^2 - \tilde{\omega}^2 - \tfrac{1}{4}\Gamma^2)^2 + \Gamma^2\delta\omega^2\,]}\ \{\ \Gamma\delta\omega\tau +$$

$$e^{-\Gamma\tau/2}\,[\ A_1 \sin(\delta\omega-\tilde{\omega})\tau + A_2 \cos(\delta\omega-\tilde{\omega})\tau$$

$$+ A_3 \sin(\delta\omega+\tilde{\omega})\tau + A_4 \cos(\delta\omega+\tilde{\omega})\tau\ ] - (A_2 + A_4)\ \} \quad (2.9)$$

$$K = \frac{4}{[\,(\delta\omega^2 - \tilde{\omega}^2 - \tfrac{1}{4}\Gamma^2)^2 + \Gamma^2\delta\omega^2\,]}\ \{\ -(\delta\omega^2 - \tilde{\omega}^2 - \tfrac{1}{4}\Gamma^2)\tau$$

$$+ e^{-\Gamma\tau/2}\,[\ -A_2 \sin(\delta\omega-\tilde{\omega})\tau + A_1 \cos(\delta\omega-\tilde{\omega})\tau$$

$$- A_4 \sin(\delta\omega+\tilde{\omega})\tau + A_3 \cos(\delta\omega+\tilde{\omega})\tau\ ] - (A_1 + A_3)\ \} \quad (2.10)$$

where

$$B_1 = \frac{-1}{\sigma} \frac{(\delta\omega^2-\sigma^2+\frac{1}{4}\Gamma^2)[(\delta\omega^2-\sigma^2+\frac{1}{4}\Gamma^2)^2+ 4\delta\omega^2\sigma^2] + 4\Gamma^2\delta\omega^2\sigma^2}{[\ (\delta\omega^2 - \sigma^2 + \frac{1}{4}\Gamma^2)^2 + 4\sigma^2\delta\omega^2\ ]} \qquad (2.17)$$

$$B_2 = \Gamma \frac{[\ (\delta\omega^2 - \sigma^2 + \frac{1}{4}\Gamma^2)^2 - 4\delta\omega^2\ (\delta\omega^2 + \frac{1}{4}\Gamma^2)\ ]}{[\ (\delta\omega^2 - \sigma^2 + \frac{1}{4}\Gamma^2)^2 + 4\sigma^2\delta\omega^2\ ]} \qquad (2.18)$$

$$B_3 = \frac{\Gamma\delta\omega}{\sigma} \frac{[\ (\delta\omega^2 - \sigma^2 + \frac{1}{4}\Gamma^2)^2 - 4\sigma^2\ (\sigma^2 - \frac{1}{4}\Gamma^2)\ ]}{[\ (\delta\omega^2 - \sigma^2 + \frac{1}{4}\Gamma^2)^2 + 4\sigma^2\delta\omega^2\ ]} \qquad (2.19)$$

$$B_4 = -2\delta\omega \frac{[\ (\delta\omega^2 - \sigma^2 - \frac{1}{4}\Gamma^2)^2 + 4\sigma^2\delta\omega^2 - \frac{1}{4}\Gamma^4\ ]}{[\ (\delta\omega^2 - \sigma^2 + \frac{1}{4}\Gamma^2)^2 + 4\sigma^2\delta\omega^2\ ]} \qquad (2.20)$$

These are the expressions used to generate Figures 3-16.

APPENDIX 3

PROPOSED EXPERIMENTAL DETECTION OF STIMULATED THOMSON SCATTERING

The following experimental proposal, and Figure 22 which illustrates it, are due to L. W. Anderson and J. E. Lawler. In order to evaluate the possibility of detecting stimulated Thomson scattering, reasonable values for certain experimental parameters must be assumed. The plasma is assumed to be produced by a pinch discharge, and to have an electron density of $n_e = 10^{15}$ cm^{-3} and an electron temperature of $k_B T_e = 10$ eV. These parameters are reasonable for a pinch discharge[71]. It is assumed that the pump laser has a pulse duration of 3 nsec and an energy per pulse of 1.0 J at a wavelength of 694.3 nm. The pump laser has a waist diameter at focus of 0.01 cm and hence a Rayleigh range of $Z_R = \frac{\pi w_o^2}{\lambda} = 4.5$ cm. The pump laser intensity at the focus is $I_o = 2.1 \times 10^{12}$ W/cm^2.

If the plasma is completely ionized (i.e. the neutral gas pressure is negligible) then the pump laser will heat the plasma primarily by inverse bremsstrahlung. The percentage increase in the electron temperature due to heating by the focussed laser beam is on the order of

5%, a tolerable perturbation to the plasma[72]. A broadband dye laser centered at wavelength 694.3 nm is used as the probe laser. The dye laser has an energy per pulse of 10^{-2} J and a pulse duration of 3 nsec. The dye laser has the same waist and Rayleigh range as the pump laser. Plasmas and lasers with these properties are available.

The peak gain coefficient is $\alpha = 2.8 \times 10^{-4}$ cm^{-1} at a wavelength of 700.4 nm with the assumed experimental parameters. Note that $v_{th}\ \omega/c$ is more than 5 times as large as the plasma frequency. The single pass gain product for the stimulated Thomson scattering is $\alpha L = \alpha Z_R = 1.3 \times 10^{-3}$. Although the gain product is small, it is possible to detect by the use of polarization enhancement as introduced by Wieman and Hänsch[73]. Polarization enhancement may provide a three order of magnitude increase in signal to background. In this situation the light transmitted by the blocking polarizer is increased by 130% above the light transmitted without stimulated Thomson scattering. With existing plasmas and lasers it should be possible to detect stimulated Thomson scattering.

The probe beam can be analyzed with a low resolution grating monochrometer and detected with a multielement detector array. The measurement of the gain for

$\lambda > 694.3$ nm or absorption for $\lambda < 694.3$ nm as a function of λ will yield both n_e and T_e for the plasma. If a 30 element array with 33% quantum efficiency were used, then each of the 30 elements would detect about 3.5×10^7 dye laser photons. This number assumes the dye laser has an energy of 10^{-2} J per pulse and assumes an extinction ratio of 10^{-7} for the crossed polarizers. If the signal to noise ratio for the detector array were limited by photon statistics, then an intensity modulation of 1.7×10^{-4} would just be detectable. This corresponds to the gain from a plasma with $n_e = 1.3 \times 10^{11} cm^{-3}$ and $T_e = 10$ eV. Stimulated Thomson scattering may be useful as a diagnostic for laboratory plasmas and arcs. One additional advantage of using stimulated Thomson scattering as a diagnostic is that spontaneous emission from the plasma would not be a major source of noise. A small gain or absorption is detected with a near diffraction limited probe laser beam. The probe laser beam is spatially filtered after traversing the plasma. Since all the stimulated photons are emitted into the same small solid angle as the probe beam, only the spontaneous emission into this small solid angle acts as a background noise source.

BIBLIOGRAPHY

1. J. J. Thomson, Conduction of Electricity Through Gases, (Cambridge: At the University Press, 1903), pp. 268-273.
2. A. Einstein, Phys. Zeit. 18, 121 (1917).
3. P. L. Kapitza and P. A. M. Dirac, Proc. Camb. Phil. Soc. 29, 297 (1933).
4. H. Dreicer, Phys. Fluids 7, 735 (1964).
5. R. H. Pantell, G. Soncini, and H. E. Puthoff, IEEE J. Quantum Electronics QE-4 11, 905 (1968).
6. J. M. J. Madey, J. Appl. Phys. 42, 1906 (1971).
7. V. P. Sukhatme and P. A. Wolff, J. Appl. Phys. 44, 2331 (1973).
8. J. R. Albritton, Phys. Fluids 18, 51 (1975).
9. W. B. Colson, Phys. Letters 59A, 187 (1976).
10. L. R. Elias, W. M. Fairbank, J. M. J. Madey, H. A. Schwettman, and T. I. Smith, Phys. Rev. Letters 36, 717 (1976).
11. D. A. G. Deacon, L. R. Elias, J. M. J. Madey, G. J. Ramian, H. A. Schwettman, and T. I. Smith, Phys. Rev. Letters 38, 892 (1977).
12. J. M. J. Madey, H. A. Schwettman, and W. M. Fairbank, IEEE Trans. Nucl. Sci. (USA) 20, 980 (1973), (Particle Accelerator Conference, San Francisco, Calif., 5-7 Mar. 1973).
13. F. A. Hopf, P. Meystre, M. O. Scully, and W. H. Louisell, Optics Commun. 18, 413 (1976).
14. A. G. Litvak and V. Yu. Trakhtengerts, Zh. Eksp. Teor. Fiz. 60, 1702 (1971), [Sov. Phys. - JETP 33, 921 (1971)].
15. A. T. Lin and J. M. Dawson, Phys. Fluids 18, 201 (1975).
16. A. Hasegawa, K. Mima, P. Sprangle, H. H. Szu, and V. L. Granatstein, Appl. Phys. Letters 29, 542 (1976).
17. F. A. Hopf, P. Meystre, M. O. Scully, W. H. Louisell, Phys. Rev. Letters 37, 1342 (1976).
18. H. A. Abawi, F. A. Hopf, and P. Meystre, Phys. Rev. 16, 666 (1977).
19. W. B. Colson, Phys. Letters 64A, 190 (1977).
20. T. Kwan, J. M. Dawson, and A. T. Lin, Phys. Fluids 20, 581 (1977).
21. S. Ichimaru and N. Iwamoto, J. Phys. Soc. Japan 44, 1004 (1978).
22. N. M. Kroll and W. A. McMullin, Phys. Rev. 17, 300 (1978).

23. M. Friedman and M. Herndon, Phys. Rev. Letters 28, 210 (1972).
24. M. Friedman and M. Herndon, Phys. Rev. Letters 29, 55 (1972).
25. M. Friedman and M. Herndon, Appl. Phys. Letters 22, 658 (1973).
26. V. L. Granatstein, M. Herndon, R. K. Parker, and S. P. Schlesinger, IEEE Trans. Microwave Theory Tech. MTT-22, 1000 (1974).
27. T. C. Marshall, S. Talmadge, and P. Efthimion, Appl. Phys. Letters 31, 320 (1977).
28. P. C. Efthimion and P. S. Schlesinger, Phys. Rev. 16, 633 (1977).
29. P. M. Platzman, S. J. Buchbaum, and N. Tzoar, Phys. Rev. Letters 12, 573 (1964).
30. N. M. Kroll, A. Ron, and N. Rostoker, Phys. Rev. Letters 13, 83 (1964).
31. M. V. Goldman and D. F. Dubois, Phys. Fluids 8, 1404 (1965).
32. V. N. Tsytovich, Nonlinear Effects in Plasma (Plenum Press, New York, 1970).
33. G. Weyl, Phys. Fluids 13, 1802 (1970).
34. P. A. Wolff, Proc. 2nd Int. Conf. on Light Scattering in Solids, 180 (Paris, 19-23 July, 1971).
35. B. I. Cohen, A. N. Kaufman, and K. M. Watson, Phys. Rev. Letters 29, 581 (1972).
36. D. W. Forslund, J. M. Kindel, and E. L. Lindman, Phys. Rev. Letters 29, 249 (1972).
37. M. N. Rosenbluth and C. S. Liu, Phys. Rev. Letters 29, 701 (1972).
38. D. W. Forslund, J. M. Kindel, and E. L. Lindman, Phys. Rev. Letters 30, 739 (1973).
39. A. N. Kaufman and B. I. Cohen, Phys. Rev. Letters 30, 1306 (1973).
40. W. L. Kruer, K. G. Estabrook, and K. H. Sinz, Nucl. Fusion 13, 952 (1973).
41. P. S. Lee, Y. C. Lee, C. T. Chang, and D. S. Chuu, Phys. Rev. Letters 30, 538 (1973).
42. G. Schmidt, Phys. Fluids 16, 1676 (1973).
43. B. I. Cohen, Phys. Fluids 17, 496 (1974).
44. J. F. Drake, P. K. Kaw, Y. C. Lee, G. Schmidt, C. S. Liu, and M. N. Rosenbluth, Phys. Fluids 17, 788 (1974).
45. W. M. Mannheimer and E. Ott, Phys. Fluids 17, 463 (1974).
46. P. Sprangle and V. L. Granatstein, Appl. Phys. Letters 25, 377 (1974).
47. P. Sprangle, J. Plasma Phys. 11, 299 (1974).

48. P. Sprangle, V. L. Granatstein, and L. Baker, Phys. Rev. 12, 1697 (1975).
49. C. S. Liu and P. K. Kaw, Advances in Plasma Physics 6, 83 (1976).
50. B. I. Cohen and A. N. Kaufman, Phys. Fluids 20, 1113 (1977).
51. B. I. Cohen and A. N. Kaufman, Phys. Fluids 21, 404 (1978).
52. P. Sprangle and V. L. Granatstein, Phys. Rev. 17, 1792 (1978).
53. P. Sprangle and A. T. Dobrot, NRL Memorandum Report 3587 (1978).
54. P. Sprangle, R. A. Smith, and V. L. Granatstein, NRL Memorandum Report 3888 (1978).
55. R. M. Kulsrud and J. Arons, Astrophys. J. 198, 709 (1975).
56. R. Weymann, Phys. Fluids 8, 2112 (1965).
57. Ya. B. Zel'dovich, and E. V. Levich, Zh. Eksp. Teor. Fiz. 55, 2423 (1968), [Sov. Phys. - JETP 28, 1287 (1969)].
58. R. A. Syunyaev, Astron. Zh. 48, 244 (1971), [Sov. Astron. AJ 15, 190 (1971)].
59. S. Johnston, Phys. Fluids 19, 93 (1976).
60. S. Johnston and R. M. Kulsrud, Phys. Fluids 20, 829 (1977).
61. S. Johnston and R. M. Kulsrud, Phys. Fluids 20, 1674 (1977).
62. W. J. Cocke, Phys. Rev. 17, 1713 (1978).
63. A. Bambini and A. Renieri, Lett. Nuovo cimento 21, 399 (1978).
64. B. I. Cohen, A. Mostrom, D. R. Nicholson, A. N. Kaufman, C. E. Max, and A. B. Langdon, Phys. Fluids 18, 470 (1975).
65. G. Schmidt, Physics of High Temperature Plasmas, (Academic Press, New York, 1966), pp.217-222.
66. G. Knorr, Plasma Phys. 11, 917 (1969).
67. A. Lee and G. Pocobelli, Phys. Fluids 15, 2351 (1972).
68. M. Abramowitz and I. A. Stegun, Handbook of Mathematical Functions (Dover Publications, Inc., New York, 1972), Chap. 16.
69. B. D. Fried and S. D. Conte, The Plasma Dispersion Function (Academic Press, New York, 1961).
70. J. Dawson, Phys. Fluids 4, 869 (1961).
71. D. J. Rose and M. Clark, Plasmas for Controlled Fusion (MIT Press, Cambridge, Mass., 1965).
72. Ya. B. Zeldovich and Yu. P. Raizer, Physics ofShock Waves and High Temperature Hydrodynamic Phenomena (Academic Press, New York, 1966).

73. C. Wieman and T. W. Hänsch, Phys. Rev. Letters 36, 1170 (1976).